Spin relaxation in polarized interacting exciton gas in quantum wells

T. Amand, D. Robart, X. Marie, M. Brousseau, P. Le Jeune, and J. Barrau
Laboratoire de Physique des Solides, CNRS URA 74, INSA, Avenue de Rangueil, 31077 Toulouse Cedex, France
(Received 10 April 1996)

Fast initial decays of both the luminescence intensity and the circular luminescence polarization, under resonant excitation of high exciton densities (typically above 2×10^{10} cm^{-2}), are reported. These fast decays, which are not observed in a dense excitonic system with well-defined angular momentum $J_z=1$ (or $J_z=-1$), are simultaneously initiated by the increase of the ellipticity of the photogenerating picosecond laser beam. We show that all the experimental observations support the driving role of the exciton-exciton exchange interaction in the spin-relaxation mechanism at high density. The theory of the mechanism is developed, leading to the simulation of luminescence and polarization dynamics for varied photogeneration conditions (intensity and polarization of the laser beam, temperature of the exciton gas). The theory provides an excellent interpretation of all the very specific features of the experimental data. The dephasing mechanism in polarized interacting exciton gas is identified. [S0163-1829(97)02515-0]

I. INTRODUCTION

The optical properties of two-dimensional (2D) excitons in quantum wells (QW's) have been the subject of extensive studies. Ten years ago, Hulin *et al.* demonstrated that, in quasi-two-dimensional systems, the exciton energy is renormalized to higher values at high densities.[1,2] The blueshift of the exciton absorption line was shown to be tied to the reduced dimensionality of excitons, being well apparent in GaAs wells of approximately 50 Å wide, but disappearing rapidly for larger well sizes.

The authors interpreted this effect in terms of a strong reduction of long-ranged many-body interaction in a 2D system, in agreement with the theoretical analysis by Schmitt-Rink, Chemla, and Miller.[3] It is well documented that in three-dimensional (3D) systems, the excitons absolute energy remains unchanged, even at high densities. This constant energy is attributed to an almost exact compensation between two many-body effects acting in opposite directions: an interparticle attraction which, for bound electron-hole pairs at $T\simeq0$ K, is similar to a van der Waals interaction between atoms, and a repulsive contribution having its origin in the Pauli exclusion principle acting on the Fermi particles (electrons and holes) forming the excitons. It has been argued by Schmitt-Rink, Chemla, and Miller that the attractive component, which can be viewed as a long-ranged Coulomb correlation effect, is strongly reduced in a 2D system, so that the short-range repulsive part now becomes unbalanced.

A few years ago, in time-resolved luminescence spectroscopy under circularly polarized and nonresonant laser beam excitation, an energy splitting has been reported between the two components of the HH1-$E1$ exciton luminescence.[4,5] The component of the same helicity as the pump laser is always at a higher energy than the other of opposed helicity. The splitting increases with the exciton density and is strongly correlated with the time evolution of the spin-polarization rate of the optically active excitons. These results were also interpreted in terms of many-body interaction within the excitonic system. The mutual Pauli repulsion of excitons photocreated by the σ^+ polarized laser beam having the same spin (presently, $J_z=+1$ excitons) is invoked to interpret the blueshift of the σ^+ polarized luminescence component.

More recently, Snelling *et al.* reported time-resolved measurements of the changes in transmission produced by excitonic saturation at various wavelengths in the vicinity of the heavy-hole exciton resonance, at room temperature.[6] They conclude that the two contributions to the exciton saturation in GaAs quantum wells, i.e., phase-space filling and Coulombic effects, were of similar magnitude.

A clear redshift of the σ^- polarized exciton line has been recognized, in time-resolved absorption[7] and luminescence[8] spectroscopy performed with a σ^+ polarized beam. This redshift indicates the action of an attractive interaction between the optically active excitons of opposed spins. In a previous work in resonant excitation conditions, we investigated the splitting of the exciton luminescence at time $t=0_+$ (i.e., immediately after the laser excitation), when the polarization of the laser beam was progressively varied from circular to linear.[9] This led us to the determination of the strengths of the repulsive and attractive parts of the interaction between the excitons. The results, which will be useful in this paper, were close to the predictions of Schmitt-Rink, Chemla, and Miller.[3]

The exciton photoluminescence (PL) dynamics has been investigated in resonant excitation conditions in very high quality GaAs/Al$_x$Ga$_{1-x}$As QWs:[10–12] after a quasi-instantaneous rise, the luminescence intensity decays over more than one order of magnitude in a characteristic time of about 20 ps, followed by a much slower decay in the order of 200 ps. The long decay time is attributed to the radiative recombination of thermalized excitons. Four contributions were proposed to interpret the short one: (a) the radiative free exciton lifetime;[11,13] (b) the exciton scattering out of the $J=1$, $k_\parallel\simeq0$ optically active states to $J=1$, $k_\parallel>0$ optically nonactive states;[10,11] (c) the relaxation of the exciton total angular momentum from the photogenerated $|1,\pm1\rangle$ states to optically nonactive $|2,\pm2\rangle$ states by hole spin flip;[10,11] (d) the recombination of biexcitons.[14,15]

In Secs. II and III we recall briefly the experimental effects already published,[16] concerning the relaxation of the luminescence intensity and of the luminescence polarization which follow the resonant photogeneration of bidimensional dense exciton gas by a picosecond laser pulse. They relate to a 60 periods of nonintentionally doped 4.8-nm GaAs wells and 15 nm $Al_{0.3}Ga_{0.7}As$ barriers grown on a (100) substrate. The shift between the ground-state heavy-hole exciton (XH) absorption peak and the XH emission peak, measured, respectively, in cw photoluminescence excitation (PLE) and PL experiments, is 6 meV. The characteristics of the laser excitation (intensity, energy, polarization) are varied in order to get information on the mechanisms of exciton-exciton scattering in the dense exciton phase ($\gtrsim 10^{10}$ cm^{-2}). Under elliptically polarized light excitation, a short decay time ($\lesssim 4$ ps) of the luminescence intensity is observed which cannot be interpreted in the known schemes (a), (b), (c), or (d).

As a matter of fact, recent experiments gave evidence of the consequences of the exciton-exciton scattering on the radiative recombination of thermalized excitons[17,18] but none of these studies considered the possibility of an associated spin-flip process. Experiments under elliptically polarized light excitation demonstrate that a new very efficient mechanism driven by the exciton-exciton spin interaction takes place at high density ($\gtrsim 2\times 10^{10}$ cm^{-2}).

Several groups have reported recently that, in GaAs quantum wells, exciton-exciton interactions are observable in transient coherent spectroscopy, as four-wave-mixing experiments.[19–22] The mechanisms by which coherence is destroyed are widely ignored however. This paper is a contribution in this field of investigations.

Theoretical models which have been proposed[23,24] to explain the exciton spin relaxation do not consider exciton-exciton interaction. The models give alternative explanations about spin relaxation in terms of intraexcitonic exchange,[23–28] Dyakonov-Perel,[29] and Elliot-Yaffet[30] -type mechanisms. We present in this paper the theory of a spin-relaxation mechanism of excitons which is controlled by the interexciton exchange interaction (Sec. IV). This mechanism dominates the initial phase of spin relaxation at high density ($\gtrsim 2\times 10^{10}$ cm^{-2}). Kinetic equations are derived in Sec. V. They yield the simulation of the main specific features of the luminescence intensity and circular polarization decays. A more achieved theory is developed in Sec. VI, which provides a clear interpretation of the experiments.

We recall the experimental conditions. The sample, in a liquid-helium bath at 1.7 K, is excited by 1.2-ps pulses generated by a tunable Ti-doped sapphire laser at a repetition rate of 80 MHz. The excitation energy is strictly resonant with the XH absorption peak and the detection energy is set to the excitonic luminescence peak. The photocreated exciton density $N(0)$, calculated from the measured spot diameter and total absorbed energy, is varied from 5×10^9 to 7×10^{10} cm^{-2}. The uncertainty on the determination of the absolute density is estimated to be $\Delta N/N=0.4$, while the relative variations of N are accurate within 2%. We checked that the spectrally integrated intensity at $t=0$ has a linear dependence on the excitation power within 10%. The PL signal is detected by the up-conversion technique using a $LiIO_3$ nonlinear crystal; the overall time resolution is thus limited by the laser temporal width. The excitation light polarization is set using a Soleil-Babinet compensator. The polarization of the excitation beam can be tuned continuously from purely circularly to purely linearly polarized light. The degree of circular polarization of the elliptically polarized excitation light beam is defined as $P_E=(\Sigma^+-\Sigma^-)/(\Sigma^++\Sigma^-)$, where Σ^+ and Σ^- denote the intensities of the right and left circularly polarized components. The degree of linear polarization of the elliptically polarized beam is defined as $P_E^{\rm lin}=(\Sigma^X-\Sigma^Y)/(\Sigma^X+\Sigma^Y)$, where Σ^X and Σ^Y denote the intensities of the X and Y linearly polarized components. To determine the circular (or linear) degree of the luminescence polarization, a rotating $\lambda/4$ (or $\lambda/2$) plate is placed before the nonlinear crystal, which acts as an analyzer. The circular and linear polarization degrees of the luminescence are defined similarly as $P_L=(I^+-I^-)/(I^++I^-)$ and $P_L^{\rm lin}=(I^X-I^Y)/(I^X+I^Y)$, where I^+, I^-, I^X, I^Y are the respective components of the luminescence.

For a (100)-grown quantum well, the relevant symmetry is D_{2d}, and the growth direction is taken as the quantization axis for the angular momentum. The conduction band is s-like, with two spin-states $s_{e,z}=\pm 1/2$. The upper valence band is split into a heavy-hole band with the total angular momentum projection $j_{h,z}=\pm 3/2$ and a light-hole band with $j_{h,z}=\pm 1/2$ at the center of the Brillouin zone. As the amplitude of the heavy-hole/light-hole splitting in the investigated samples is much greater than the exciton binding energy, as well as the exciton thermal energy in resonant experiments, the heavy-hole exciton states will be described using only the heavy-hole subspace, with the basis set $|J_z\rangle=|j_{h,z},s_{e,z}\rangle$, i.e., $|J_z=1\rangle\equiv|3/2,-1/2\rangle$, $|J_z=-1\rangle\equiv|-3/2,1/2\rangle$, $|J_z=2\rangle\equiv|3/2,1/2\rangle$, $|J_z=-2\rangle\equiv|-3/2,-1/2\rangle$. Here $\mathbf{J}$ and J_z represent the total angular momentum of the exciton and its projection on the quantization axis, respectively. This basis set is diagonal with respect to the exciton exchange interaction, and the twofold degenerate $J=1$ states are split from the twofold $J=2$ states by the electron-hole exchange energy. In this representation, it is obvious that heavy excitons with $J=1$ are dipole allowed and those with $J=2$ are forbidden for optical transitions. The two-dimensional subset of dipole-allowed states can be described in terms of an exciton effective spin as usual. The light propagation being parallel to the quantum well's growth axis, we take the same quantization axis for photons and excitons. Circularly polarized photons σ^+ and σ^- will create, respectively, $|+1\rangle$ and $|-1\rangle$ exciton states with equal probabilities. So the extension to elliptically (or linearly) polarized photons is straightforward: when heavy-hole excitons are excited resonantly with elliptically polarized light (P_E), the excitons are created in states $|\psi_\theta\rangle$, which are expressed as linear superpositions of $|+1\rangle$ and $|-1\rangle$ states, with coefficients corresponding to the light ellipticity ($P_E=\sin 2\theta$):

$$|\psi_\theta\rangle=\frac{\cos\theta+\sin\theta}{\sqrt{2}}|+1\rangle+\frac{\cos\theta-\sin\theta}{\sqrt{2}}|-1\rangle, \qquad (1)$$

with $-\pi/2<\theta\leqslant+\pi/2$. We refer to these exciton states as elliptic excitons in the following. Excitons in states $|X\rangle=|\psi_0\rangle$ and $|Y\rangle=|\psi_{\pi/2}\rangle$, photogenerated with X-polarized and Y-polarized light, respectively, are called linear excitons. Excitons in states $|\psi_{\pi/4}\rangle$ and $|\psi_{-\pi/4}\rangle$, photogenerated with σ^+ and σ^- polarized light, are called circular excitons. An ellip-

tic exciton is characterized by its circular and linear polarization degree, respectively, $P_\theta = \sin 2\theta$ and $P_\theta^{\text{lin}} = \cos 2\theta$.

II. LUMINESCENCE DECAY

We investigate first the total excitonic luminescence dynamics. We showed previously that time-resolved PL experiments, using different degrees of circular polarization of the excitation light, is a very powerful tool to investigate the exciton formation and the complex behavior of the exciton depolarization dynamics.[31] Presently, we apply this procedure to the study of the luminescence dynamics in resonant excitation conditions.

Figure 1(a) presents the PL intensity variation during the first 40 ps for an initial exciton density $N(0)=2\times10^{10}$ cm^{-2} and $P_E=50\%$. It is well known for resonant excitation, that the risetime of the luminescence is extremely fast (limited by our instrument response time), in contrast with the long rise time (>100 ps) observed for nonresonant excitation.[32] The monoexponential decrease is slow, characterized by a decay time τ_x^{rad} of about 300 ps measured in an experiment performed on a larger time range. As expected, the fast free exciton lifetime (which is about 20 ps) is not observed in QWs with interface defects,[33] whose presence is revealed here by the Stokes shift of 6 meV. Figure 1(a) displays also the result of the same experiment for a higher created exciton density $N(0)=7\times10^{10}$ cm^{-2}. The striking difference is that the luminescence decay is not monoexponential now: the intensity drops by about a factor 2 within 5 ps and then decays much more slowly. This factor of 2 suggests that this surprising effect, i.e., the initial fast luminescence decay, is directly connected to the exciton relaxation between $J_z=\pm1$ and $J_z=\pm2$ states. In Fig. 1(b), we observe step by step on the same point of the sample that this initial fast decay time, absent at low exciton density, is more and more pronounced as the photocreated exciton density is raised from 2×10^{10} to 5×10^{10} cm^{-2}. A saturation of the effect is observed however: the fast drop by a factor close to 2 shown in Fig. 1(a) was the maximum that could be observed. Above the photogeneration density of 7×10^{10} cm^{-2} the trend is rather a decrease of the relative intensity of the initial spike of luminescence. These observations suggest that the initial short decay time has its origin in a collective phenomenon.

Several authors state strong biexcitonic effects in GaAs quantum wells at low temperature.[14,15,34–36] In the experiment reported by Wang *et al.*,[14] excitons are excited resonantly by linearly polarized laser pulses (120 fs temporal width). The authors attribute the cross-polarized luminescence to biexcitons, assuming that biexcitons are created resonantly through the two-photon absorption process. They conclude to an extremely fast decay (3 ps) of the biexciton into a photon and an exciton. Nevertheless in their photogeneration conditions, the copolarized excitonic luminescence always dominates. Our laser excitation conditions (picosecond pulses, elliptic polarization) are rather less propitious for dominant biexcitonic effects. However a definitive conclusion cannot be pronounced at this moment. We will see in the next section that the circular polarization of the luminescence dynamics can rule out this biexcitonic effect hypothesis.

In order to further investigate this initial short decay time, we performed a series of experiments with a fixed initial exciton density $N(0)=5\times10^{10}$ cm^{-2}, but with different P_E values, from 32% to 100%, Fig. 1(c). The fast initial drop of the luminescence intensity is not observed for $P_E=100\%$. It begins to be visible for $P_E=80\%$ and then becomes more and more pronounced as P_E decreases; the associated decay

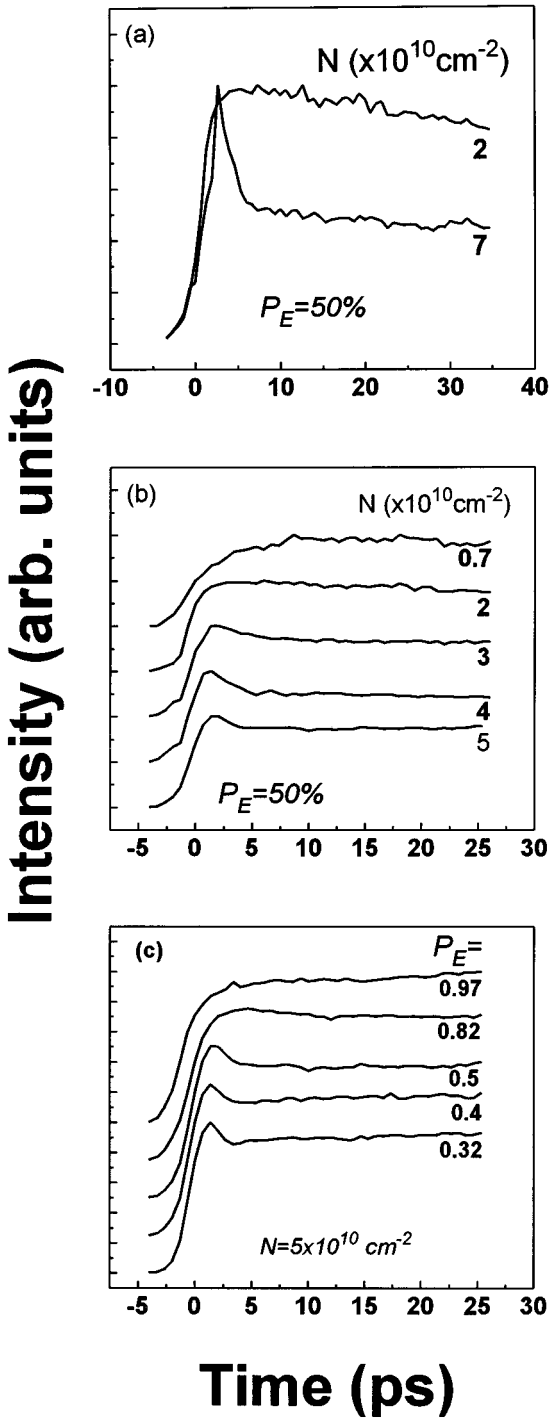

FIG. 1. (a) Normalized total luminescence intensity at $N(0)=2\times10^{10}$ and 7×10^{10} cm^{-2}; $P_E=50\%$ in both cases. (b) Normalized total luminescence intensity for $P_E=50\%$. From the top to the bottom, we have indicated the estimated initial exciton density $N(0)$ in units of 10^{10} cm^{-2}. (c) Normalized total luminescence intensity at $N(0)=5\times10^{10}$ cm^{-2} and for different P_E (from 32% to 97%).

time decreases when P_E decreases. This behavior definitively rules out an interpretation of the short decay time based either on the fast radiative exciton lifetime as in Refs. 11, 13, or on the exciton scattering from $J=1$, $k_{\|}\simeq 0$ optically active states to $J=1$, $k_{\|}>0$ optically nonactive states,[10,11] a process not expected here since the energy to dissipate ($\sim$6 meV) from the exciton absorption peak to the emission peak is higher than the lattice thermal energy $k_B T_L$ (a fast initial luminescence intensity drop due to this process is only observed in very high quality samples—i.e., without Stokes shift—in which the resonantly photocreated excitons are colder than the lattice).

The same experiment performed at low excitation densities [$N(0)<2\times10^{10}$ cm^{-2}] shows that there is no initial fast decay of the PL intensity whatever the P_E value is. Furthermore, under pure circularly polarized excitation ($P_E=100\%$), when the excitation density is raised up to $N(0)=7\times10^{10}$ cm^{-2}, no initial fast decay time is observed in the exciton time-resolved luminescence.

The conclusion of the preceding analysis of the luminescence dynamics is that the fast initial decay exists only at *high density* [$N(0)\gtrsim 2\times10^{10}$ cm^{-2}] when a population of *elliptic* excitons is photogenerated ($P_E\neq 100\%$). This suggests that the transfer from optically active to optically nonactive exciton states is initiated by the interaction between excitons resulting from an elliptic photogeneration ($P_E<100\%$). The efficiency of this transfer is an increasing function of the ellipticity *and* of the density.

III. CIRCULAR DEPOLARIZATION

We investigate now the luminescence circular polarization dynamics. The intensity and the polarization of the laser beam are varied again. Figure 2(a) shows the time evolution of the right I^+ and left I^- circularly polarized luminescence intensities and the corresponding decay of the circular polarization degree of the luminescence $P_L(t)$ at high exciton density $N(0)=5\times10^{10}$ cm^{-2} when $P_E=35\%$. The results with $P_E=50\%$ are similar. The luminescence polarization dynamics has clearly two components. With a decay time of 5 ps, the polarization drops from 35 to 10%. From investigations with longer time delays, we find that the remaining polarization decreases in this case, with a decay time of about 35 ps. Moreover, Fig. 2(a) shows clearly that this fast polarization decay and the fast luminescence decay ($I^+ + I^-$) occur simultaneously.

This observation definitively rules out the interpretation in terms of fast radiative recombination of biexcitons.[14,15] Biexcitons are known as combinations of two excitons $|+1\rangle$ and $|-1\rangle$.[12] The biexciton luminescence process leaves one photon and one exciton of opposite helicity. If the initial spike of luminescence was due to the radiative recombination of biexcitons it would be unpolarized, the $|+1\rangle$ and $|-1\rangle$ components decaying at the same rate. Therefore, a fast decay of biexciton luminescence would correspond to an increase of the circular polarization. This is in contradiction with the experiment which shows a fast circular polarization decay starting at $P_L(0)=P_E$ (cf. all the recordings shown in Fig. 2).

Figure 2(b) illustrates the density dependence of the circular polarization dynamics for $P_E=35\%$. The fast initial

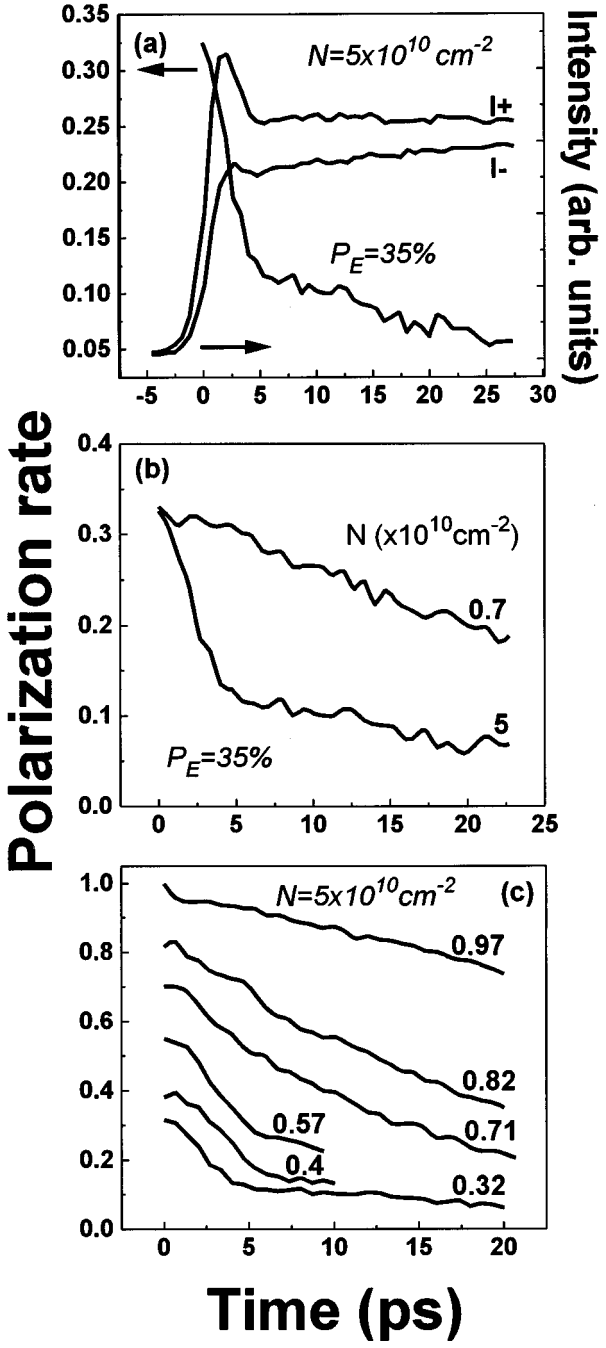

FIG. 2. (a) Luminescence intensities $I^+(t)$, $I^-(t)$, and circular polarization $P(t)$ at $N(0)=5\times10^{10}$ cm^{-2} and $P_E=35\%$. (b) Time evolution of $P_L(t)$ at $N(0)=7\times10^9$ and 5×10^{10} cm^{-2} when $P_E=35\%$. (c) Time evolution of $P_L(t)$ at different P_E from 32% to 97% when $N(0)=5\times10^{10}$ cm^{-2}.

decay is less and less pronounced as the photocreated exciton density decreases. Below $N(0)=2\times10^{10}$ cm^{-2}, the circular polarization decays monoexponentially with a time constant of 35 ps, regardless of the value of P_E. This last value is in good agreement with the calculated exciton spin relaxation time T_{s1} (the so-called *longitudinal spin relaxation time*), due to both exchange interaction between the electron and the hole within the exciton and spin-orbit interaction for the hole.[23] The conclusion is that a very efficient new spin-relaxation mechanism takes place at high density.

In order to further investigate this new spin-relaxation

mechanism, we also analyze the role of P_E by performing experiments at a fixed high exciton density but different P_E values, as in Sec. II. Figure 2(c) presents the results at $N(0)=5\times10^{10}$ cm^{-2}.

(i) For $P_E=100\%$, there is no initial fast decay of P_L; the decay time is the ''slow decay time'' ($\sim$35 ps).

(ii) When $P_E<100\%$ the initial acceleration of the depolarization is observed and the corresponding decay time decreases when P_E decreases.

When it occurs, the fast circular depolarization dynamics exhibits two very unusual features which can be used as critical tests for a theory (Fig. 2).

(i) The fast depolarization stops before the full depolarization; then a slow dynamics follows.

(ii) The fast depolarization begins with a downward curvature.

The conclusion of this analysis of the circular depolarization dynamics is that the fast initial decay of the circular polarization exists only at *high density* when a population of *elliptic excitons* is photogenerated. It is striking that these two conditions are identical to those which drive the fast initial drop of the luminescence intensity already discussed in Sec. II. Moreover we notice that the fast initial circular-polarization decay always coincides with the fast initial drop of the luminescence intensity: it is clearly observed in Fig. 2(a). This suggests that both phenomena are related to the same exciton-exciton scattering mechanism.

IV. ROLE OF THE EXCHANGE INTERACTION BETWEEN EXCITONS

The conclusion of the experiments on luminescence and circular-polarization dynamics is that their simultaneous fast decay appears when a population of elliptic excitons is photogenerated at high density. In principle, in an ideal experiment where one photon is absorbed, the electron-hole pair should preserve the polarization state $|\psi_\theta\rangle$ in which it is created, the electron-hole spin correlation being held by the electron-hole exchange interaction. But as soon as several photons are absorbed, the exchange interaction between the excitons, which can reach several millielectron volt at high density,[9] affects their stability. At high density, this interaction becomes stronger than the electron-hole exchange within the exciton, destroying the internal spin correlation. The efficiency of this mechanism depends on the ellipticity of the occupied states $|\psi_\theta\rangle$. This is analyzed now in details.

First, examine the structure of the different terms describing the exciton-exciton exchange interaction. In D_{2d} symmetry, the heavy-hole exciton is made of a Γ_6 electron with $|s_{e,z}=\pm1/2\rangle$ as basis states, and a Γ_6 hole with $|j_{h,z}=\pm3/2\rangle$. The spin operator s_z belongs to the Γ_2, while (s_x,s_y) belongs to the Γ_5 representation. Introducing an effective heavy-hole spin $\tilde{s}_h=1/2$ and identifying the $|j_{h,z}=+3/2\rangle$ with the $|\tilde{s}_{h,z}=+1/2\rangle$ state and $|j_{h,z}=-3/2\rangle$ with $|\tilde{s}_{h,z}=-1/2\rangle$, symmetry considerations allow us to describe the e-e and h-h spin-spin couplings representing the exchange between two excitons (designated as i and j hereafter) by the effective Hamiltonian:

$$\mathcal{H}^{i,j}_{e\text{-}e}=a_e s^i_{e,z}s^j_{e,z}+b_e(s^i_{e,x}s^j_{e,x}+s^i_{e,y}s^j_{e,y}), \tag{2a}$$

$$\mathcal{H}^{i,j}_{h\text{-}h}=a_h\tilde{s}^{\,i}_{h,z}\tilde{s}^{\,j}_{h,z}+b_h(\tilde{s}^{\,i}_{h,x}\tilde{s}^{\,j}_{h,x}+\tilde{s}^{\,i}_{h,y}\tilde{s}^{\,j}_{h,y}). \tag{2b}$$

Whereas the parameters a_e and a_h are expected of the same order, b_h is much smaller than b_e, in principle, since it corresponds to a second-order effect resulting from the mixing to the light-hole subband: in the limit of vanishing mixing (large splitting between the heavy- and light-hole subbands) we should have $b_h=0$. In the following we neglect b_h in comparison with b_e. Moreover, because of the different symmetries of conduction- and valence-band wave functions, the e-h term of the exciton-exciton exchange interaction is smaller and can be totally ignored. Finally, the total spin-spin coupling between two excitons is approximated as

$$\mathcal{H}^{i,j}\simeq a_e s^i_{e,z}s^j_{e,z}+a_h\tilde{s}^{\,i}_{h,z}\tilde{s}^{\,j}_{h,z}+\frac{b_e}{2}(s^i_{e,+}s^j_{e,-}+s^i_{e,-}s^j_{e,+}). \tag{3}$$

Now we adopt the convention that $s^i_{e,\lambda}$ and $\tilde{s}^{\,i}_{h,\lambda}$ are the Pauli spin operators. The interaction of two excitons is described by the action of $\mathcal{H}^{i,j}$ on their exciton pair state. Then, the three following equations provide the basis for the interpretation of the observed phenomena:

$$\mathcal{H}^{i,j}|\psi_\theta\rangle^i|\psi_\theta\rangle^j=(a_e+a_h)|\psi_{\pi/2-\theta}\rangle^i|\psi_{\pi/2-\theta}\rangle^j + b_e\sqrt{2}\,\cos2\theta\left(\frac{|2\rangle^i|\overline{2}\rangle^j+|\overline{2}\rangle^i|2\rangle^j}{\sqrt{2}}\right), \tag{4a}$$

$$\mathcal{H}^{i,j}|1\rangle^i|\overline{1}\rangle^j=-(a_e+a_h)|1\rangle^i|\overline{1}\rangle^j+2b_e|2\rangle^i|\overline{2}\rangle^j, \tag{4b}$$

$$\mathcal{H}^{i,j}|2\rangle^i|\overline{2}\rangle^j=-(a_e+a_h)|2\rangle^i|\overline{2}\rangle^j+2b_e|1\rangle^i|\overline{1}\rangle^j. \tag{4c}$$

Equation (4a) indicates that exchange interaction between two elliptic excitons results in the transfer to the optically passive states but *preserves the circular polarization* degree of the optically active phase since $\psi_{\pi/2-\theta}$ and ψ_θ excitons have the same circular polarization.[37] This instability is a real specificity of elliptically polarized excitonic phases: the transfer rate, which takes the form

$$k_1(1-\sin^2 2\theta)N^2_\theta, \quad \text{where } k_1\propto 2|b_e|^2$$

is zero in a purely circularly polarized exciton system ($\theta=\pm\pi/4$) and is maximum in a purely linearly polarized one ($\theta=0$ or $\pi/2$).[38]

Assuming that coherence is lost in the first transfer to the optically passive subspace, the study of binary interactions within the optically passive subsystem needs to consider the operation of $\mathcal{H}^{i,j}$ on the three different two-exciton states $|2\rangle^i|\overline{2}\rangle^j$, $|\overline{2}\rangle^i|2\rangle^j$, and $|2\rangle^i|2\rangle^j$ successively. States $|2\rangle^i|2\rangle^j$ and $|\overline{2}\rangle^i|\overline{2}\rangle^j$, in which the two excitons have the same orientation, are stable for the same reason as $|1\rangle^i|1\rangle^j$ but scattering can occur when $|2\rangle$ and $|\overline{2}\rangle$ excitons interact. Equation (4c) shows that this interaction produces optically active excitons with *equal probabilities* for the two opposed helicities $|+1\rangle$ and $|-1\rangle$. The rate of transfer is

$$2k_2N_2N_{\overline{2}}=\frac{k_2}{2}(N_{J=2})^2 \quad \text{where } k_2=k_1\propto 2|b_e|^2. \tag{5}$$

We reach here the mechanism of the *fast circular depolarization* observed quasisimultaneously with the fast transfer to the optically passive subspace [Fig. 2(a)].

On the contrary, in a mixed population of $|+1\rangle$ and $|-1\rangle$ excitons, the transfer to the optically nonactive states depopulates the $|+1\rangle$ and $|-1\rangle$ states at the same rate [Eq. 4(b)] resulting in the relative increase of the dominant helicity, i.e., in a *repolarization*. In this case, the depolarization effect associated with the reverse process [Eq. 4(c)] cannot counterbalance the repolarization associated with the direct transfer [Eq. 4(b)] since $|\pm 2\rangle$ states are not initially populated. The overall result is then a repolarization of the luminescence, while there is always depolarization for an elliptic exciton system.

All the preceding simple considerations about the mechanism of the exciton-exciton exchange interaction give the true qualitative support to the conclusions of Secs. II and III relative to the conditions of the observation of the simultaneous initial fast decays of both luminescence intensity and circular polarization.

As soon as reactions described by Eqs. (4a) and (4c) progress, states $|\psi_{\pi/2-\theta}\rangle$, $|\pm 1\rangle$, and $|\pm 2\rangle$ are populated. In order to develop a quantitative theory leading to the kinetic equations which control the luminescence intensity and polarization dynamics it is necessary to examine all the possible binary interactions that can occur then within the excitonic system. Consider successively reactions between the optically active and the optically passive excitonic subsystems (i) and within the optically active subsystem itself (ii).

(i) The first class of reactions is described by

$$\mathcal{H}^{i,j}|\psi_\theta\rangle^i|\pm 2\rangle^j = \mp(a_e - a_h)|\psi_{\pi/2-\theta}\rangle^i|\pm 2\rangle^j + b_e|\pm 2\rangle^i|\psi_\theta\rangle^j \pm b_e|\pm 2\rangle^i|\psi_{\pi/2-\theta}\rangle^j. \quad (6)$$

This equation shows that exchange interaction between an optically active and an optically passive exciton does not modify the circular polarization nor the intensity of the excitonic luminescence.

(ii) The second class of reactions is described by

$$\mathcal{H}^{i,j}|\psi_{\theta'}\rangle^i|\psi_{\theta''}\rangle^j = (a_e + a_h)|\psi_{\pi/2-\theta'}\rangle^i|\psi_{\pi/2-\theta''}\rangle^j + b_e\sqrt{2}\cos(\theta' + \theta'')\left(\frac{|2\rangle^i|\overline{2}\rangle^j + |\overline{2}\rangle^i|2\rangle^j}{\sqrt{2}}\right) + b_e\sqrt{2}\sin(\theta' - \theta'')\left[\frac{|2\rangle^i|\overline{2}\rangle^j - |\overline{2}\rangle^i|2\rangle^j}{\sqrt{2}}\right]. \quad (7)$$

The transfer to states $|\psi_{\pi/2-\theta}\rangle$, described by the first term in the second member, does not change the circular polarization nor the intensity of the luminescence. The transfer to the optically passive subspace, described by the two other terms, occurs at the rate

$$k_1(1-\sin 2\theta' \times \sin 2\theta'')N_{\theta'}N_{\theta''} \quad \text{where} \quad k_1 \propto 2|b_e|^2. \quad (8)$$

N_θ denotes the density of excitons occupying states $|\psi_\theta\rangle$. Equation (7) shows moreover that the transfer probabilities towards states $|+2\rangle$ and $|-2\rangle$ are equal. This principle of equal population of states $|+2\rangle$ and $|-2\rangle$ can easily be checked in all the reactions.

If we consider now the exchange splitting between optically active and optically passive exciton states, measured by ε_{ex}, the necessity of agreement with the detailed balance principle provides the relation $k_2 = k_1 \exp(-2\varepsilon_{ex}/k_B T)$.

Conditions for the modelization of the recorded luminescence and polarization dynamics are now collected. Two levels of approximation shall be examined successively in Secs. V and VI.

V. KINETIC EQUATIONS WITHOUT RENORMALIZATION OF THE EXCITON ENERGY

A. Kinetic equations

For the sake of simplicity, we do not consider in this first approach the possible corrections resulting from renormalization of the exciton energy in the interacting exciton gas. We wish to obtain the kinetic equations describing the dynamics related to the exchange interaction between the excitons. Consequently, we ignore all other spin-relaxation mechanisms and recombination. Consider the photogeneration of N excitons at time $t=0$, by an elliptically polarized laser beam (P_E). We imagine the optically active subsystem, at the time t of the relaxation, as an assembly of excitons distributed on different elliptic states ψ_θ. We denote $N_\theta \equiv N(\theta, t)$ this distribution hereafter. The density of optically active excitons and the circular polarization of the associated luminescence at time t, are, respectively,

$$N_{J=1} = \sum_\theta N_\theta \quad (9a)$$

and

$$P_L = \frac{\sum_\theta N_\theta \sin 2\theta}{N_{J=1}}. \quad (9b)$$

Initial conditions are

$$N_{J=1}(t=0) = N, \quad P_L(t=0) = P_E. \quad (10)$$

The decay rates of density and circular polarization of optically active excitons (the measured observables) are expressed as

$$\frac{dN_{J=1}}{dt} = -\frac{dN_{J=2}}{dt} = \sum_\theta \frac{dN_\theta}{dt}, \quad (11a)$$

$$\frac{1}{P_L}\frac{dP_L}{dt} = -\frac{1}{N_{J=1}}\frac{dN_{J=1}}{dt} + \frac{1}{P_L N_{J=1}}\sum_\theta \sin 2\theta \frac{dN_\theta}{dt}. \quad (11b)$$

The decay rate of the density N_θ is evaluated according to Eqs. (5) and (8):

$$\frac{dN_\theta}{dt} = -k_1 \sum_{\theta'} (1-\sin 2\theta \sin 2\theta') N_\theta N_{\theta'} + \frac{k_2}{2} (N_{J=2})^2 \delta_{\sin 2\theta, \pm 1}$$

$$= -k_1 (1 - P_L \sin 2\theta) N_\theta N_{J=1} + \frac{k_2}{2} (N_{J=2})^2 \delta_{\sin 2\theta, \pm 1}. \quad (12)$$

Equations which control the decays of the luminescence intensity and of the circular polarization of the luminescence are obtained by the substitution of Eq. (12) into (11):

$$\frac{dN_{J=1}}{dt} = -k_1 (1-P_L^2)(N_{J=1})^2 + k_2 (N_{J=2})^2, \quad (13a)$$

$$\frac{dN_{J=2}}{dt} = -\frac{dN_{J=1}}{dt}, \quad (13b)$$

$$\frac{1}{P_L}\frac{dP_L}{dt} = -\frac{1}{N_{J=1}}\frac{dN_{J=1}}{dt} - k_1 \sum_{\theta'} N_{\theta'} \cos^2 2\theta'. \quad (13c)$$

In Eq. (13c), the two contributions are positive (first term) and negative (second term), respectively, the second being the very specific contribution of elliptic excitons (for pure circular excitons, $\cos^2 2\theta' = 0$). This means that the fast circular depolarization relate unambiguously to the presence of elliptic excitons within the optically active excitonic subsystem. When these metastable excitons anihilate, the second contribution cancels and the fast circular depolarization stops. Then the system moves slowly towards a quasistationary repartition of the excitons between the $J=1$ and 2 subsystems satisfying the condition:

$$1 - P_L^2 = \frac{k_2}{k_1} \left(\frac{N_{J=2}}{N_{J=1}} \right)^2. \quad (14)$$

This quasiequilibrium corresponds to a stationary solution for the system (13). Then, the circular polarization increase, related to the transfer of a pair of $|+1\rangle$ and $|-1\rangle$ excitons to the $J=2$ subsystem, is strictly balanced by the transfer of a pair from the $J=2$ subsystem, which becomes optically active in the two opposed helicities. The observation of the fast circular depolarization is the first very specific feature of the experimental recordings previously noticed. The present theory predicts also the second unusual feature i.e., the initial downward curvature of the fast circular-depolarization signal, Fig. 2: this is shown by an initial slope equal to zero, according to Eq. (13c).

B. Coherence relaxation

Elliptic excitons, which express as linear combinations of states $|\pm 1\rangle$, are *coherent states*. All the coherent states contribute additively to the second term in the second member of Eq. (13c) and their presence in the excitonic phase is revealed by the recording of the fast circular depolarization. So far, we merely interpreted the exciton-exciton exchange interaction in terms of transition probabilities (Sec. IV), assuming that coherence memory was definitively lost as elliptic excitons transfer to the nonoptically active subspace. This is a reasonable hypothesis for an *energy nonconserving* process. Therefore, we considered that excitons come back on optically active states $|+1\rangle$ and $|-1\rangle$ exclusively [cf. Eq. (4c)]. Consequently the optically active excitons distribute only on three states at any time t of the decay: the elliptic photogeneration state $|E\rangle \equiv |\psi_\theta\rangle$, characterized by $\sin 2\theta = P_E \neq \pm 1$, and the pure circular states $|+1\rangle$ and $|-1\rangle$. The decay of the coherence term in Eq. (13c) is then fully related to the decay of the density of excitons on the photogeneration states $N_E(t)$ due to their transfer to the $J=2$ optically nonactive subspace. The formulation is

$$\sum_{\theta'} N_{\theta'} \cos^2 2\theta' = (1-P_E^2) N_E(t), \quad (15a)$$

with

$$\frac{dN_E}{dt} = -k_1 (1 - P_E P_L) N_E N_{J=1}. \quad (15b)$$

The energy-conserving transitions towards $|\psi_{\pi/2-\theta}\rangle$ [Eqs. (6), (7)], a state which has the same circular polarization as $|\psi_\theta\rangle$, have not been considered explicitly here because excitons $|\psi_{\pi/2-\theta}\rangle$ and $|\psi_\theta\rangle$ contribute identically to the circular polarization P_L and behave identically with respect to the transfer to optically nonactive states [cf. Eq. (8)]. For these reasons, both populations are considered together in N_E. This should be different if the problem was the evaluation of the linear polarization dynamics.

The full set of Eq. (13) is rewritten as

$$\frac{dN_{J=1}}{dt} = -k_1 (1-P_L^2)(N_{J=1})^2 + k_2 (N_{J=2})^2, \quad (16a)$$

$$\frac{dN_{J=2}}{dt} = -\frac{dN_{J=1}}{dt}, \quad (16b)$$

$$\frac{1}{P_L}\frac{dP_L}{dt} = -\frac{1}{N_{J=1}}\frac{dN_{J=1}}{dt} - k_1 (1-P_E^2) N_E, \quad (16c)$$

$$\frac{dN_E}{dt} = -k_1 (1 - P_E P_L) N_E N_{J=1}. \quad (16d)$$

The coherence decay-time depends on the photogenerating conditions (N, P_E) and is strongly time dependent.

C. Simulation of the experiments

Considering that P_E is fixed by the excitation conditions, the numerical solution of (16) for $N_{J=1}(t)$ and $P_L(t)$ depends on the reaction constant k_1 only. The constant $k_2 = k_1 \exp -2\varepsilon_{ex}/k_B T$ is deduced taking $\varepsilon_{ex} = 0.15$ meV for the $GaAs/Ga_xAl_{1-x}As$ quantum well (well width 4.8 nm), a choice in agreement with the experimental measurements reported in Ref. 39; T is the exciton temperature.

The simulations of the experimental data, which results from the numerical resolution of Eq. (16) using the four points Runge-Kutta method, are displayed in Figs. 3 and 4. Here, the exciton photogeneration is modelized by a very short squared hyperbolic secant pulse (FWHM $= \tau_{pulse} = 0.2$ ps), so short that exciton-exciton interactions which occur

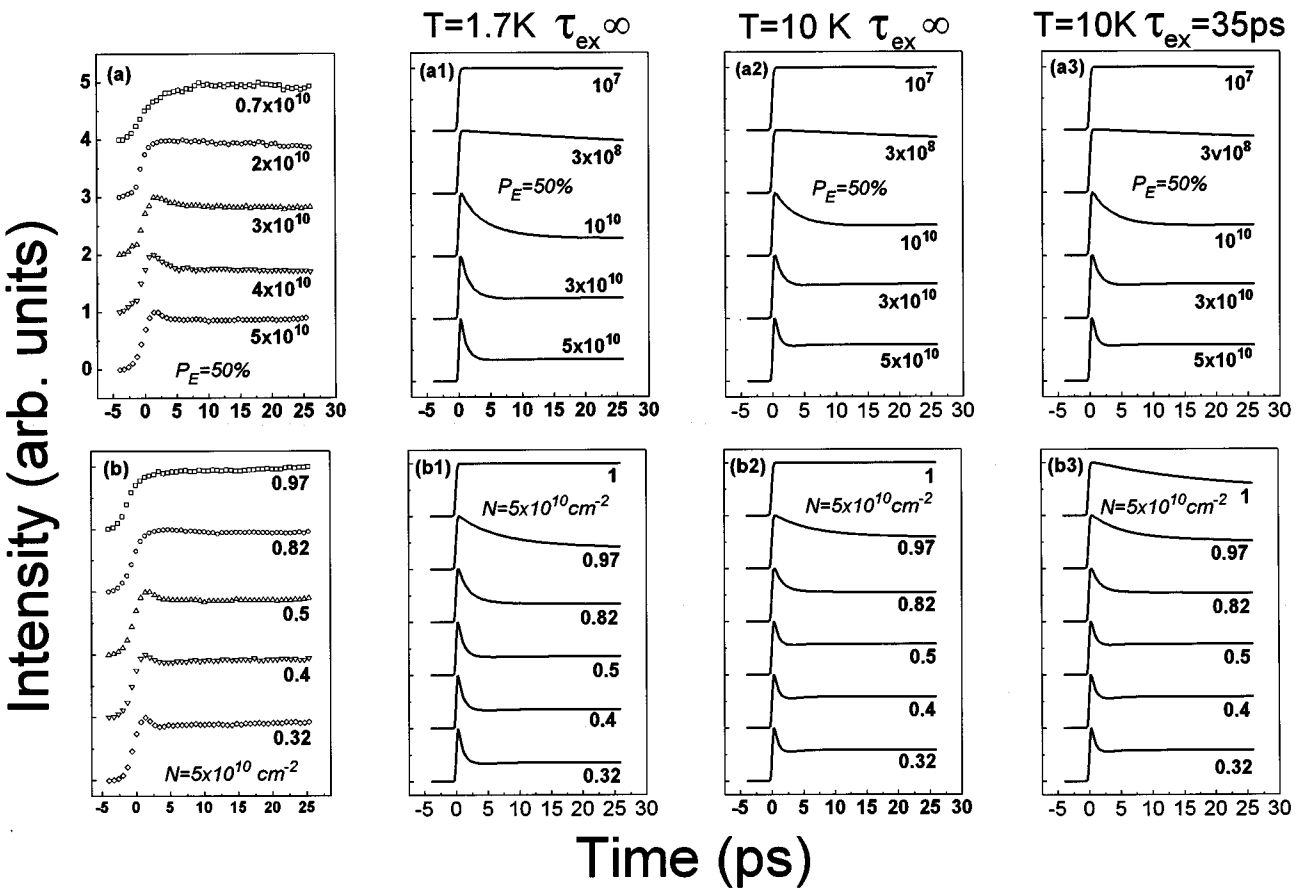

FIG. 3. (a) and (b) duplicate Figs. 1(b), 1(c). The simulations displayed in columns 2, 3, 4, correspond to the three combinations of parameters given in the Table I.

during the pulse have negligible consequences (the actual experimental pulse width will be introduced in a second step). The values chosen for the parameters k_1 and T are reported in the Table I. The experimental recordings of Figs. 1(b), 1(c), and 2(b), 2(c) are reproduced in the first column of Figs. 3 and 4, respectively, for comparison. Figures 3(a)–3(a3) and 4(a)–4(a3) illustrate the effect of varying the density N at a fixed laser polarization P_E. Figures 3(b)–3(b3) and 4(b)–4(b3) illustrate the effect of varying the polarization P_E at a fixed density N. Columns 2 and 3 correspond to two different temperatures, 1.7 and 10 K, respectively, i.e., lower and higher than $T_{\mathrm{ex}}=2\varepsilon_{\mathrm{ex}}/k_B\simeq 4$ K. Column 4 illustrates the effect of adding the extra term $-1/\tau_{\mathrm{ex}}$ with $\tau_{\mathrm{ex}}=35$ ps in the second member of Eq. (16c) in order to include the consequences of the intraexciton exchange spin-flip mechanism.

Actually, the reaction constant has been chosen in order to get the best similitude with the experimental data recorded at the highest density (5×10^{10} cm^{-2}). The comparison between theory and experiment leads us to the two following remarks.

(i) The theory provides a good description of the phenomenon. The main features of the luminescence and circular-polarization dynamics, as well as the density-and polarization-dependent trends, are well expressed by the theory. We emphasize that the very specific experimental features arise from the effect of a single parameter, the reaction constant k_1.

(ii) The observed phenomenon develops on a smaller density range than predicted theoretically. We interpret this experimental behavior as the consequence of the localization of excitons at low density, an expected effect in the present sample.[40] The exciton-exciton exchange interaction is a specificity of extended exciton states for which the center-of-mass wave functions overlap. When the photogenerated density is of the order or lower than the exciton traps density, we expect that luminescence arises entirely from localized excitons for which the short-range mutual exchange interaction is switched off. It follows that the vanishing of the fast decays when $N\lesssim 2\times10^{10}$ cm^{-2} is consistent with an exciton traps density of the order 2×10^{10} cm^{-2}. It should be very interesting to perform similar experiments on a high quality sample, characterized by a negligible Stokes shift. The experiment would require however in this case two synchronized laser sources of different wavelengths, in order to perform resonant excitation.

Figure 5 illustrates the consequences of increasing, in the simulation, the photogenerating pulse width to the actual experimental value. The experimental recordings are reported again in the left column for an easier comparison. Simulations with $\tau_{\mathrm{pulse}}=0.2$ and 1.5 ps are displayed in columns 2 and 3, respectively. When $\tau_{\mathrm{pulse}}=1.5$ ps, the transfer towards the optically dark states begins during the pulse itself at high density. The main consequence is a progressive smoothing of the initial spike of luminescence when the density increases, in agreement with the experiment (it was reported in Sec. II that, above $N=7\times10^{10}$ cm^{-2}, the trend is to the decrease of the relative intensity of the initial fast luminescence decay). The increase of the pulse width has minor consequences on the polarization dynamics.

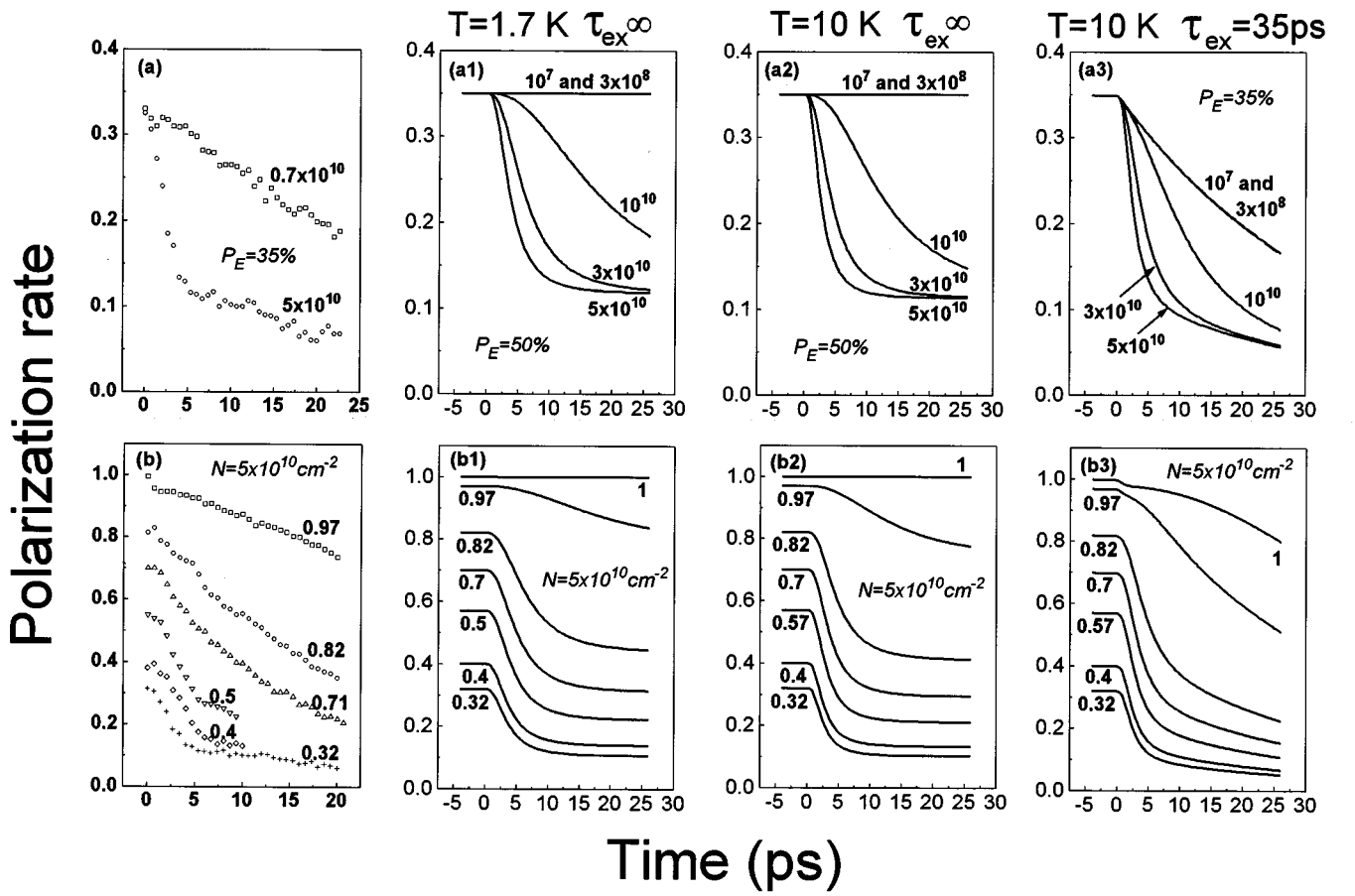

FIG. 4. (a) and (b) duplicate Figs. 2(b), 2(c). The simulations displayed in columns 2, 3, 4 correspond to the three combinations of parameters given in the Table I.

D. Repolarization of a mixed population of $|+1\rangle$ and $|-1\rangle$ excitons

One can photogenerate directly such a mixed population by focusing colinearly two-pulsed laser beams of opposed helicities but avoiding coherent coupling. Practically, the two beams are split from the same primary picosecond laser source but an additional delay, larger than the exciton dephasing time, is attributed to one of them. The possibility of photogeneration of elliptic excitons is ruled out in this way.

The first (second) pulse generates σ^+ (σ^-) excitons at density N_1 (N_1^-). Taking the time origin ($t=0$) at the arrival of the second pulse the total exciton density is almost $N(0)=N_1+N_1^-$, with polarization $P_L(0)=(N_1-N_1^-)/N$. The second term in the second member of (16c) vanishes. The integration is then straightforward. The result is

$$N_{J=1}(t)=N(0)\,\frac{P_L(0)}{P_L(t)},\quad N_{J=2}(t)=N(0)\left[1-\frac{P_L(0)}{P_L(t)}\right]. \tag{17}$$

The transient initiated by the arrival of the second pulse corresponds to the increase of circular polarization which results from the immediate transfer of excitons pairs of opposed helicities from the optically active subspace to the optically nonactive one. This transfer vanishes when a quasistationnary equilibrium still verifying Eq. (14) is reached. A fast luminescence decay accompany necessarily this transfer. The circular polarization saturates at the value obtained by combination of Eqs. (14) and (17):

$$P_L(\infty)=P_L(0)\,\frac{k_2/k_1+\sqrt{(1-k_2/k_1)[P_L(0)]^2+k_2/k_1}}{[P_L(0)]^2+k_2/k_1}. \tag{18a}$$

TABLE I. The parameters used for the resolution of Eq. (16) leading to the simulation of the luminescence decays and the circular-polarization decays displayed in Figs. 3, 4, and 5, respectively.

	Figs. 3 and 4 (a_1,b_1)	Figs. 3 and 4 (a_2,b_2)	Figs. 3 and 4 (a_3,b_3)	Fig. 5 (a_1,b_1)	Fig. 5 (a_2,b_2)
k_1	20 cm^2/s	20 cm^2/s	20 cm^2/s	20 cm^2/s	20 cm^2/s
T	1.7 K	10 K	10 K	10 K	10 K
τ_{pulse}	0.2 ps	0.2 ps	0.2 ps	0.2 ps	1.5 ps
τ_{ex}	∞	∞	35 ps	35 ps	35 ps

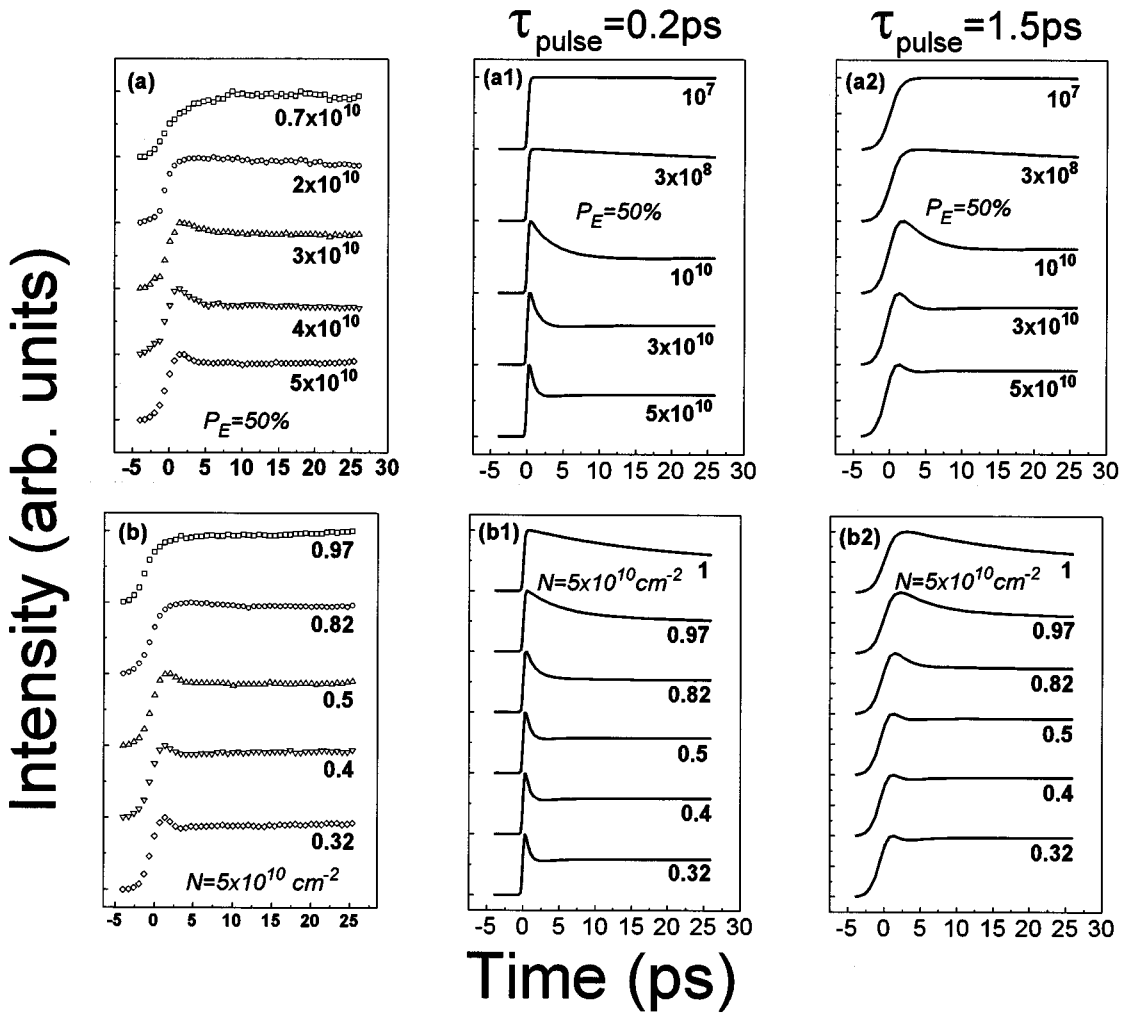

FIG. 5. Illustration of the effect of increasing the photogenerating pulse width in the simulation of the circular-polarization dynamics.

This value is between the ''high-temperature'' and ''low-temperature'' limits,

$$k_B T \gg 2\varepsilon_{\rm ex}, \quad P_L(\infty) = \frac{2P_L(0)}{1+[P_L(0)]^2}, \tag{18b}$$

$$k_B T \ll 2\varepsilon_{\rm ex}, \quad P_L(\infty) = 1. \tag{18c}$$

We emphasize the prediction of a full repolarization of the excitonic luminescence at the lower temperatures [Eq. (18c)]. We performed this two pulses (σ^+, σ^-) experiment. We do observe such a repolarization. These results shall be analyzed at the end of Sec. VI.

VI. KINETIC EQUATIONS WITH RENORMALIZATION OF THE EXCITON ENERGY

A. Renormalized rate constant

In a dense and polarized exciton gas, a spin-dependent renormalization of exciton states which can reach several meV occurs. In the present case, where the $|+2\rangle$ and $|-2\rangle$ spin states are equally occupied, positions on the energy scale are [Appendix B, Eq. (B4)]

$$\mathcal{E}_\theta = (\langle a_e\rangle + \langle a_h\rangle)(1 + P_L \sin 2\theta) N_{J=1} + (\langle a_e\rangle + \langle a_h\rangle) N_{J=2} - K_2 N + \varepsilon_{\rm exc}, \tag{19a}$$

$$\mathcal{E}_{\pm 2} = [(\langle a_e\rangle + \langle a_h\rangle) \mp (\langle a_e\rangle - \langle a_h\rangle) P_L] N_{J=1} + (\langle a_e\rangle + \langle a_h\rangle) N_{J=2} - K_2 N. \tag{19b}$$

Index θ, ± 2 refer to the different spin states $|\psi_\theta\rangle$ (which include $\theta = \pm\pi/4$) and $|\pm 2\rangle$. The $K_2 N$ term, in each equation, represents the contribution of the weak attractive part of the exciton-exciton interaction of the van der Waals type: here, for the sake of simplicity, it is assumed spin independent. The exchange splitting between $J=1$ and 2 exciton states is also taken into account. Equation (19a) is well supported by the experiment.[9]

Actually, the transfer of an exciton pair induced by the exciton-exciton exchange interaction corresponds to a ''potential-energy variation'' denoted $\varepsilon_p \equiv \varepsilon_p^{xx}$ in the following. We recall the reactions which govern the population evolution with the introduction of this potential-energy variation:

$$\text{exciton } |\psi_\theta\rangle + \text{exciton } |\psi_{\theta'}\rangle \xrightarrow{\varepsilon_p^{\theta,\theta'}} \text{exciton } |2\rangle + \text{exciton } |\overline{2}\rangle, \tag{20a}$$

$$\text{exciton } |2\rangle + \text{exciton } |\overline{2}\rangle \xrightarrow{\varepsilon_p^{2,\overline{2}}} \text{exciton } |1\rangle + \text{exciton } |\overline{1}\rangle, \tag{20b}$$

where

$$\varepsilon_p^{\theta,\theta'} \equiv (\mathcal{E}_2 + \mathcal{E}_{\bar{2}}) - (\mathcal{E}_\theta + \mathcal{E}_{\theta'}) = -\frac{K_1}{2}(\sin 2\theta + \sin 2\theta') P_L N_{J=1} - 2\varepsilon_{\rm ex},$$

$$\varepsilon_p^{\bar{2},\bar{2}} \equiv (\mathcal{E}_1 + \mathcal{E}_{\bar{1}}) - (\mathcal{E}_2 + \mathcal{E}_{\bar{2}}) = 2\varepsilon_{\rm ex}. \quad (21)$$

Here, $K_1 = 2(\langle a_e \rangle + \langle a_h \rangle)$ is a positive constant representing the strength of the repulsive part of the interaction between excitons having the same spin (like $|+1\rangle$ and $|+1\rangle$), which takes its origin in the Pauli exclusion principle.

In Sec. IV 1, both spin-dependent renormalization and exciton motion were ignored. They are considered now, which compel us to treat the problem of transition probabilities in detail. Actually, an exciton state is fully determined when both the internal state—presently the spin state $|\psi_\theta\rangle$ or $|\pm 2\rangle$—and the mass center motion—specified by the momentum **K**—are given. For instance, $|\psi_\theta\rangle|\mathbf{K}\rangle$ refer to an elliptic exciton of momentum **K**. In the exchange Hamiltonian, amplitudes a_e, a_h, b_e are now considered as a function of $r = |\mathbf{r}_1 - \mathbf{r}_2|$, the distance between the centers of mass of excitons 1 and 2. Consider the example of reaction (20b). The transition probability per unit time for a specific exciton pair transfer is written as follows:

$$\frac{2\pi}{\hbar} |\langle \mathbf{K}_i + \mathbf{Q}_i, \mathbf{K}_j + \mathbf{Q}_j | ({}^j\langle \bar{2}|^i \langle 2|\mathcal{H}^{i,j}|1\rangle^i |\bar{1}\rangle^j) |\mathbf{K}_i, \mathbf{K}_j\rangle|^2 \times \delta(\varepsilon_p + \varepsilon_{\rm kin}). \quad (22)$$

$\mathbf{K}_i$, $\mathbf{K}_j$ and $\mathbf{K}_i + \mathbf{Q}_i$, $\mathbf{K}_j + \mathbf{Q}_j$ are momentum of excitons i and j before and after the transfer, respectively, while $\varepsilon_{\rm kin}$ is the corresponding kinetic-energy variation of the exciton pair:

$$\varepsilon_{\rm kin} = \frac{\hbar^2}{2M}|\mathbf{K}_i + \mathbf{Q}_i|^2 + \frac{\hbar^2}{2M}|\mathbf{K}_j + \mathbf{Q}_j|^2 - \frac{\hbar^2}{2M}|\mathbf{K}_i|^2 - \frac{\hbar^2}{2M}|\mathbf{K}_j|^2 = \frac{\hbar^2}{M}(\mathbf{K}_i \cdot \mathbf{Q}_i + \mathbf{K}_j \cdot \mathbf{Q}_j) + \frac{\hbar^2}{2M}(|\mathbf{Q}_i|^2 + |\mathbf{Q}_j|^2). \quad (23)$$

Considering then the spin parts of matrix elements previously derived in Sec. IV and assuming a Boltzman distribution function for the exciton momentum of the form $f(\mathbf{K}) = \exp -\beta K^2$ with $\beta = \hbar^2/2Mk_BT$ (M is the exciton mass and T the exciton temperature), the rate constant for any reaction like Eq. (20) is expressed as a function of ε_p in the form

$$k(\varepsilon_p) = \frac{2\pi}{\hbar}(4\pi\beta)^2 \sum_{\mathbf{K}_i,\mathbf{K}_j} e^{-\beta(K_i^2+K_j^2)} \sum_{\mathbf{Q}_i,\mathbf{Q}_j} |\langle \mathbf{K}_i + \mathbf{Q}_i, \mathbf{K}_j + \mathbf{Q}_j | \sqrt{2} b_e(r) | \mathbf{K}_i, \mathbf{K}_j \rangle|^2 \delta(\varepsilon_p + \varepsilon_{\rm kin}). \quad (24)$$

Considering reactions (20) and their associated potential-energy variations $\varepsilon_p^{\theta,\theta'}$ or $\varepsilon_p^{\bar{2},\bar{2}}$, the reaction constants for the transfers are denoted $k^{\theta,\theta'} \equiv k(\varepsilon_p^{\theta,\theta'})$, $k^{\bar{2},\bar{2}} \equiv k(\varepsilon_p^{\bar{2},\bar{2}})$, respectively. The kinetic equation which generalizes Eq. (12) follows:

$$\frac{dN_\theta}{dt} = -\sum_{\theta'} k^{\theta,\theta'}(1 - \sin 2\theta \sin 2\theta') N_\theta N_{\theta'} + \frac{k^{\bar{2},\bar{2}}}{2}(N_{J=2})^2 \delta_{\sin 2\theta, \pm 1}. \quad (25)$$

All details on the calculation of the reaction constant $k(\varepsilon_p)$, as expressed by Eq. (24), are given in the Appendix A. The final result depends on the choice of the interexcitonic potential $b_e(r)$. Following Landau in the problem of two hydrogen atoms,[41] the asymptotic decrease of the envelope wave functions of excitons, leads to the form

$$b_e(r) = b_{e0} e^{-r/\lambda\sqrt{2}}. \quad (26)$$

It leads to the result [Eq. (A8)]:

$$k(\varepsilon_p) = k_0(|\varepsilon_p|) \times \frac{1}{1 + \exp(\varepsilon_p/k_BT)}, \quad (27a)$$

where

$$k_0(|\varepsilon_p|) = \frac{4\pi^2\hbar}{M} \frac{b_{e0}^2}{\varepsilon_\lambda^2} \frac{1 + \exp -|\varepsilon_p|/k_BT}{(1 + |\varepsilon_p|/\varepsilon_\lambda)^3} \times I(\zeta;\xi). \quad (27b)$$

$I(\zeta;\xi)$ is an integral expressed in (A8b) with a low-temperature limit equal to 1. For the range of temperatures which was explored in our research of the best fit of the experimental data, the integral $I(\zeta;\xi)$ remained very close to unity. The parameters are defined as

$$\varepsilon_\lambda = \hbar^2/2M\lambda^2, \quad \zeta = \frac{|\varepsilon_p|}{\varepsilon_\lambda}, \quad \xi = \frac{|\varepsilon_p|}{k_BT}. \quad (28)$$

The form (27a) respects the detailed balance principle. The result (27a), (27b) shows that the potential-energy variation in the transfer is paid by a reduction of the probability, *independent of the sign* of the variation: in the low-temperature limit, this reduction accounts for the factor $(1 + |\varepsilon_p|/\varepsilon_\lambda)^{-3}$.

B. Coherence relaxation

We come back to our precedent hypothesis concerning the relaxation of coherences (Sec. V B). Here, the optically active excitons, initially created with the same ellipticity (P_E), are assumed to lose their coherence suddenly and completely as they transfer to the optically nonactive states. Consequently, optically active excitons are all distributed, at the time t, on the three states $|+1\rangle$, $|-1\rangle$, and $|E\rangle \equiv |\psi_\theta\rangle$, the circular polarization of which are $+1$, -1, and $P_E = \sin 2\theta \neq \pm 1$, respectively. The kinetic equations for the densities N_1, $N_{\bar{1}}$, and N_E are derived from the general form (25). Adding the equation for $N_{J=2}$, i.e., $dN_{J=2}/dt = -d(N_1 + N_{\bar{1}} + N_E)/dt$, the full set is written as follows:

$$\frac{dN_1}{dt} = -2k^{1,\bar{1}} N_1 N_{\bar{1}} - k^{E,1}(1 - P_E) N_1 N_E + \frac{k^{\bar{2},\bar{2}}}{2}(N_{J=2})^2, \quad (29a)$$

$$\frac{dN_{\bar{1}}}{dt} = -2k^{1,\bar{1}} N_1 N_{\bar{1}} - k^{E,\bar{1}}(1 + P_E) N_{\bar{1}} N_E + \frac{k^{\bar{2},\bar{2}}}{2}(N_{J=2})^2, \quad (29b)$$

$$\frac{dN_E}{dt} = -k^{E,E}(1-P_E^2)N_E^2 - k^{E,\bar{1}}(1+P_E)N_E N_{\bar{1}} - k^{E,1}(1-P_E)N_E N_1, \tag{29c}$$

$$\frac{dN_{J=2}}{dt} = -4k^{1,\bar{1}}N_1 N_{\bar{1}} - 2k^{E,1}(1-P_E)N_1 N_E - 2k^{E,\bar{1}}(1+P_E)N_{\bar{1}} N_E - k^{E,E}(1-P_E^2)N_E^2 + k^{2,\bar{2}}(N_{J=2})^2, \tag{29d}$$

where the four rate constants $k^{E,E}$, $k^{E,\pm 1}$, $k^{1,\bar{1}}$, $k^{2,\bar{2}}$, as expressed by (27), depend on the potential-energy variations $\varepsilon_p^{x,x}$ derived from (21):

$$\varepsilon_p^{E,E} = -K_1 P_E P_L N_{J=1} - 2\varepsilon_{\rm ex},$$

$$\varepsilon_p^{E,\pm 1} = K_1 \frac{\mp 1 - P_E}{2} P_L N_{J=1} - 2\varepsilon_{\rm ex},$$

$$\varepsilon_p^{1,\bar{1}} = -\varepsilon_p^{2,\bar{2}} = -2\varepsilon_{\rm ex}. \tag{30}$$

C. Fit of the experiment

It appears that the quality of the fit is improved when the intraexcitonic exchange spin flip is taken into account. For simplicity we consider the low-density contributions to the decay rates of N_1, $N_{\bar{1}}$, N_E:

$$\left.\frac{dN_1}{dt}\right]_{\rm ex} = -\frac{1}{2\tau_{\rm ex}}\left(N_1 - N_{\bar{1}} - \frac{1-P_E}{2}N_E\right), \tag{31a}$$

$$\left.\frac{dN_{\bar{1}}}{dt}\right]_{\rm ex} = -\frac{1}{2\tau_{\rm ex}}\left(N_{\bar{1}} - N_1 - \frac{1+P_E}{2}N_E\right), \tag{31b}$$

$$\left.\frac{dN_E}{dt}\right]_{\rm ex} = -\frac{N_E}{2\tau_{\rm ex}}. \tag{31c}$$

These contributions must be added to the second member of Eqs. (29a), (29b), (29c), respectively. For the sake of simplicity we keep the intraexciton exchange relaxation-time value $\tau_{\rm ex}=35$ ps, measured at low excitation (the impact of the interexciton interactions on $\tau_{\rm ex}$ is another problem that is out of the scope of this paper). The numerical solution of (29) leads to the components $I^+(t)$ and $I^-(t)$ of the luminescence:

$$I^+(t) \propto N_1 + N_E(1+P_E)/2, \quad I^-(t) \propto N_{\bar{1}} + N_E(1-P_E)/2. \tag{32}$$

The luminescence and the circular polarization dynamics, $I^+(t)+I^-(t)$ and $(I^+-I^-)/(I^++I^-)$, respectively, are deduced then. The best fit of the experimental data are shown in Fig. 6. First, consider the data recorded at a constant photogeneration density but different laser beam polarizations, Figs. 6(b1) and 6(b2). The measured photogenerated density ($N=5\times10^{10}$ cm^{-2}) and successive laser beam polarizations, the measured pulse width ($\tau_{\rm pulse}=1.5$ ps), are taken in the simulation. We maintain our preceding choice for the intraexcitonic exchange splitting, $\varepsilon_{\rm ex}=0.15$ meV. For the Pauli repulsion constant, we take the value $K_1=2\times10^{-10}$ meV$\times$cm^2 in agreement with a previous measurement on the same sample.[9] Simulations at $T>T_{\rm ex}=2\varepsilon_{\rm ex}/k_B\simeq 4$ K turn to be slightly better; we take $T=10$ K. The remaining parameters b_{e0} and ε_λ, which characterize the exciton-exciton exchange interaction [cf. Eqs. (A7a) and (28), $b_e(r)=b_{e0}\exp -r\sqrt{M\varepsilon_\lambda/\hbar^2}$], result from the fit; the best values are

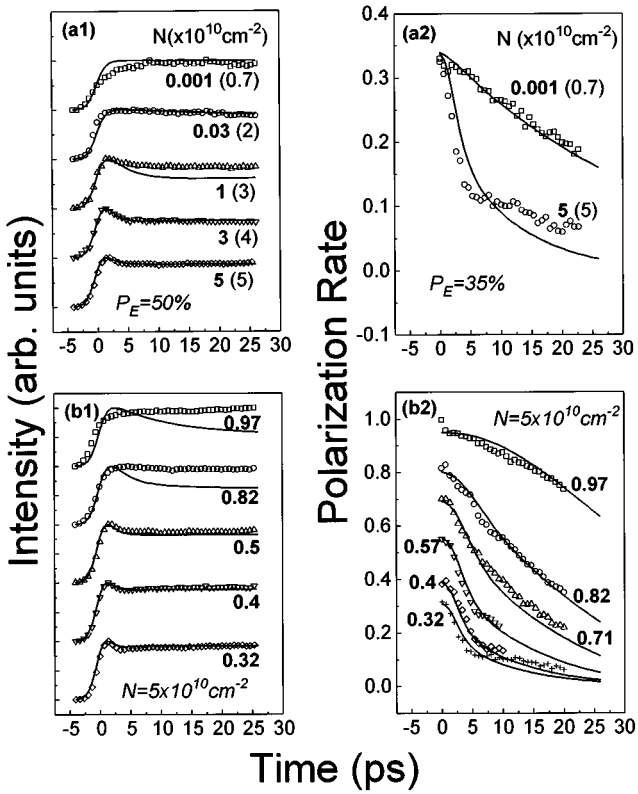

FIG. 6. (a1), (a2): the experimental luminescence and circular-polarization dynamics (symbols) at different exciton densities but constant laser beam polarization and their best simulation when the density N is considered as the fitting parameter (full lines). The resulting values are mentioned on each recording; the experimental values are reported between brackets. (b1), (b2): the experimental luminescence and circular-polarization dynamics (symbols) at different laser beam polarizations but constant exciton density and their best simulation (full lines).

$$b_{e0}=6 \text{ meV}, \quad \varepsilon_\lambda = 10 \text{ meV}. \tag{33}$$

The fact that the best fit is achieved for an exciton temperature appreciably higher than the lattice temperature is not really surprising. First, we recall that our samples exhibit a Stokes shift, so that excitons have to relax some kinetic energy. Second, even in samples without measurable Stokes shift, an intrinsic exciton heating mechanism has been reported at high exciton density.[42]

It is instructive to observe that the value of 10 meV found for ε_λ corresponds to $\lambda=38$ Å, which is of the order of the 2D exciton Bohr radius. This confirms the short-range character of the exciton-exciton exchange interaction.

The model leads to a very good simulation of most of the data. Insufficiencies are limited to the two intensity decays recorded at the highest laser polarization, i.e., when the fast transfer to the nonoptically active states is less efficient. We believe that this discrepancy is related to the exciton local-

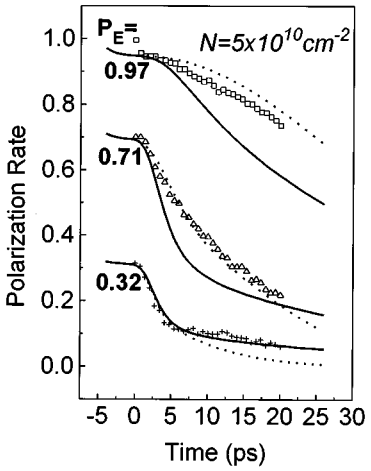

FIG. 7. Illustration of the effect of renormalization on the quality of the fit. For example, three circular-polarization dynamics are simulated with $K_1=0$ (full lines) and $K_1=3\times10^{-10}$ meV cm^2 (dotted lines) successively. Symbols reproduce the experiment.

ization. But the actual evaluation of all the consequences of this phenomenon is a difficult task which is beyond the scope of this paper.

The fits of the luminescence and polarization decays recorded at a fixed polarization of the excitation [Figs. 1(b) and 2(b)] are shown in Figs. 6(a1) and 6(a2). The parameters are the same as in the preceding simulation [Figs. 6(b1) and 6(b2)]. The measured laser polarization is taken in the simulation $P_E=50\%$ and 35%, respectively. But now, the exciton density N is considered as the fitting parameter. The best values are reported in the data. They become much lower than the actual photogenerated densities (indicated in the brackets) when the threshold of the effect is approached. As discussed previously in Sec. V C, this is the direct consequence of the localization of excitons. The densities which lead to the best fits must be considered as representative of the fraction of free excitons.

The improvement of the fit resulting from the consideration of the renormalization consequences is illustrated in Fig. 7 where the best simulations of three polarization dynamics obtained with $K_1=0$ (renormalization neglected) and $K_1=3\times10^{-10}$ meV$\times$cm^2 are compared. The optimum value $K_1=2\times10^{-10}$ meV$\times$cm^2 was taken in Fig. 6. The improvement provided by the consideration of the renormalization effect is the most obvious for experiments performed with the highest polarizations.

D. Repolarization of a mixed population of $|+1\rangle$ and $|-1\rangle$ excitons

The theory predicts a repolarization when a mixed population of $|+1\rangle$ and $|-1\rangle$ excitons is created. The experimental conditions are achieved in a two-pulses (σ^+,σ^-) excitation experiment when the delay Δt between the two pulses is long enough, so that any coherent coupling between the two photogenerated populations is excluded (c.f. Sec. V C). The results reported in Fig. 8 are recorded from the same point of the sample, taking $\Delta t=10$ ps. The total photogenerated density $N=N_1+N_1^-$ increases from a to c. Simultaneous fast luminescence decay and repolarization follow the second

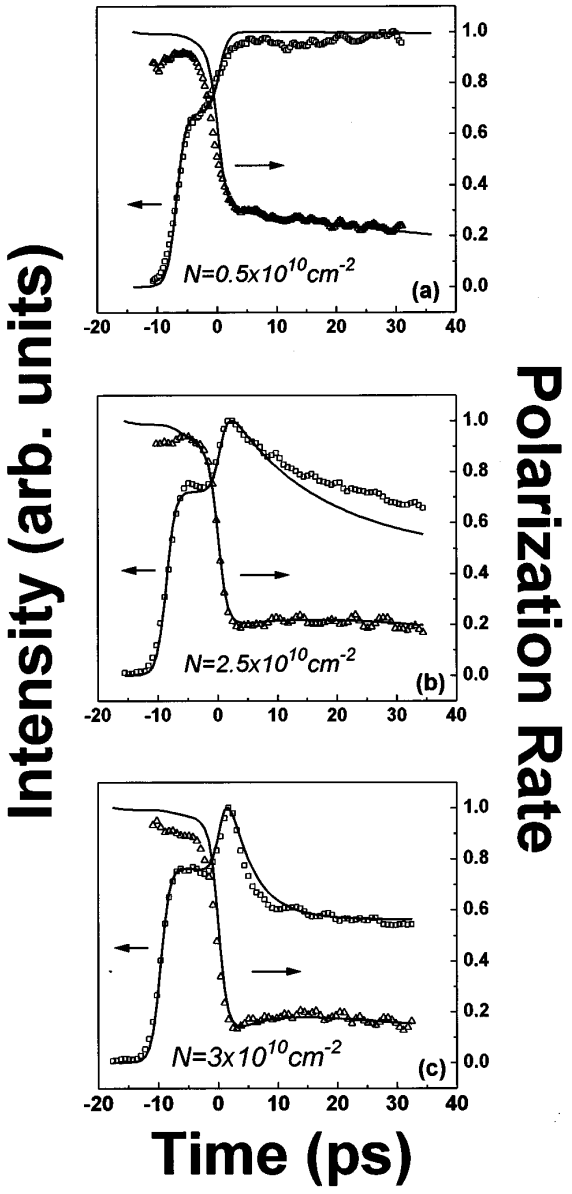

FIG. 8. The two-pulses excitation experiment (σ^+,σ^-) for $\Delta t=10$ ps. The pulse peak positions are $t=-10$ ps for σ^+ and $t=0$ for σ^-. The exciton temperature is taken $T=5$ K. □: the experimental luminescence intensity $I^+(t)+I^-(t)$; △: the experimental circular polarization $P_L(t)$. The full lines result from simulations in the following conditions: the values of the parameters are the same as in Figs. 6(b1) and 6(b2); the repartition N_1/N_1^- between $|+1\rangle$ and $|-1\rangle$ exciton states is fixed by the experiment; the total density $N=N_1+N_1^-$ is chosen in order to obtain the best fit.

	Measurement (cm^{-2})		
	N_1	N_1^-	$N=N_1+N_1^-$
(a)	3.4×10^9	1.6×10^9	0.5×10^{10}
(b)	1.6×10^{10}	0.9×10^{10}	2.5×10^{10}
(c)	1.7×10^{10}	1.3×10^{10}	3×10^{10}
	Simulation (cm^{-2})		
(a)	6.8×10^6	3.2×10^6	10^7
(b)	1.92×10^9	1.08×10^9	3×10^9
(c)	6.8×10^9	5.2×10^9	1.2×10^{10}

pulse in Figs. 8(b) and 8(c), i.e., at densities $N=2.5\times10^{10}$ and 3×10^{10} cm^{-2}, respectively. Such effects are not observed at $N=0.5\times10^{10}$ cm^{-2} [Fig. 8(a)] and lower densities. Simulations, based on Eqs. (31)–(34), are performed in the same conditions as in Figs. 6(a1) and 6(a2); the values of the parameters are the same; the repartition N_1/N_1^- between $|+1\rangle$ and $|-1\rangle$ exciton states is fixed by the experiment; the total density $N=N_1+N_1^-$ is chosen in order to obtain the best fit. Similar differences with the measured values as in Figs. 6(a1) and 6(a2) are noticed: this is again the effect of the exciton localization. With this reserve, we observe that the theory provides an appropriate prediction of the repolarization effect.

VII. CONCLUSION

When HH_1-E_1 excitons are excited resonantly with an elliptically polarized laser beam, they are created on states which are expressed as a linear superposition of $|+1\rangle$ and $|-1\rangle$, with coefficients corresponding to the light ellipticity. We have studied the depolarization processes which occur during the free relaxation of such an excitonic phase at high density. The stability of the phase is investigated, as a function of the ellipticity and intensity of the picosecond laser beam. The fast luminescence decays and fast circular-polarization decays, which appear when the ellipticity of the laser beam excitation decreases ($P_E<1$), illustrate the driving role of the exciton-exciton exchange interaction in the spin-relaxation mechanism at high density.

We have developed a theory of the exciton spin relaxation in a gas of polarized interacting excitons in which the spin flip is driven by the exciton-exciton exchange interaction. The renormalization of excitonic states has been taken into account. Kinetics equations have been derived. They allow us to reproduce all the very specific features of luminescence and circular-polarization decays for the variety of experimental photogenerating conditions and provide very satisfying fits of the data. The mechanism responsible for the coherence relaxation in dense excitonic phases is elucidated: it corresponds to the transfer of the photogenerated excitons to the optically nonactive states, a process driven by the exciton-exciton exchange interaction.

The theory predicts again a fast luminescence decay, but accompanied with a repolarization, when a mixed population of $|+1\rangle$ and $|-1\rangle$ excitons is photogenerated. The effect, which has been observed, has also been simulated.

The coherence relaxation phenomena reported in this paper are strongly related to the ''dephasing processes'' as measured in four-waves-mixing experiments performed at high excitation density.[18] However, in a gas of polarized interacting excitons the dephasing processes are expected to include not only the transfer of excitons to the optically nonactive states (i.e., the specific contribution to the fast decays reported in this paper), but also the transfer to optically active states with crossed linear polarization, a mechanism which is described by Eq. (4a)—more generally by Eq. (7)—and Eq. (6). These additional contributions are certainly extremely efficient at high density ($\sim10^{10}$ cm^{-2} and above).

Note added in proof. We have performed very recently experiments on high-quality homogeneous quantum wells (without Stokes shift) under resonant excitation, using an optical parametric oscillator synchronously pumped by the sapphire:Ti laser. The very specific features of the luminescence dynamics are again observed. This experiment confirms the present theory of exciton-exciton spin scattering.

ACKNOWLEDGMENTS

It is a pleasure for us to acknowledge V. Thierry-Mieg for the growth of the samples. We acknowledge support from CEE under the HCM Network Contract No. ERBCHRXCT 940464.

APPENDIX A

Calculation of the reaction constant $k(\varepsilon_p)$

The reaction constant for exciton transfers between the $J=1$ and 2 excitonic subspaces is expressed by Eq. (24).

(i) *The matrix-element* is first calculated:

$$M_{\mathbf{Q}_i,\mathbf{Q}_j}=\langle \mathbf{K}_i+\mathbf{Q}_i,\mathbf{K}_j+\mathbf{Q}_j|b_e(r)|\mathbf{K}_i,\mathbf{K}_j\rangle,$$

$$M_{\mathbf{Q}_i,\mathbf{Q}_j}=\int e^{-i\mathbf{Q}_i\cdot\mathbf{r}_i}e^{-i\mathbf{Q}_j\cdot\mathbf{r}_j}b_e(r)d^2r_i d^2r_j=\int e^{-i(\mathbf{Q}_i+\mathbf{Q}_j)\cdot\mathbf{r}_i}d^2r_i\int e^{-i\mathbf{Q}_j\cdot\mathbf{r}}b_e(r)d^2r. \tag{A1a}$$

Finally, we obtain

$$|M_{\mathbf{Q}_i,\mathbf{Q}_j}|^2=\delta_{\mathbf{Q}_i,-\mathbf{Q}_j}|b_e(Q_j)|^2,\quad \text{with } b_e(Q_j)=\int e^{-i\mathbf{Q}_j\cdot\mathbf{r}}b_e(r)d^2r. \tag{A1b}$$

(ii) *The sum* $S=\Sigma_{\mathbf{Q}_i,\mathbf{Q}_j}|\langle \mathbf{K}_i+\mathbf{Q}_i,\mathbf{K}_j+\mathbf{Q}_j|\sqrt{2}b_e(r)|\mathbf{K}_i,\mathbf{K}_j\rangle|^2\delta(\varepsilon_p+\varepsilon_{\rm kin})$:

$$S=2\sum_{\mathbf{Q}_i,\mathbf{Q}_j}\delta_{\mathbf{Q}_i,-\mathbf{Q}_j}|b_e(Q_j)|^2\delta\left[\varepsilon_p+\frac{\hbar^2}{M}(\mathbf{K}_i\cdot\mathbf{Q}_i+\mathbf{K}_j\cdot\mathbf{Q}_j)+\frac{\hbar^2}{2M}(|\mathbf{Q}_i|^2+|\mathbf{Q}_j|^2)\right]$$

$$=2\int_0^\infty\frac{Q\,dQ}{4\pi^2}|b_e(Q)|^2\int_0^{2\pi}d\varphi\;\delta\left(\varepsilon_p+\frac{\hbar^2|\mathbf{K}_i-\mathbf{K}_j|Q}{M}\cos\theta+\frac{\hbar^2Q^2}{M}\right)$$

$$=2\int_0^\infty\frac{Q\,dQ}{4\pi^2}|b_e(Q)|^2\int_{u^-}^{u^+}\frac{2\,\delta(u)}{\sqrt{-(u-u_+)(u-u_-)}}\,du$$

$$=2\int_0^\infty\frac{Q\,dQ}{4\pi^2}|b_e(Q)|^2\times\begin{cases}2/\sqrt{-u_+u_-} & \text{if } u=0\in\,]u_-,u_+[\\ 0 & \text{if } u=0\notin\,]u_-,u_+[.\end{cases}$$

The index in $\mathbf{Q}_j$ has been dropped. We have defined $u_\pm=\pm\hbar^2|\mathbf{K}_i-\mathbf{K}_j|Q/M+(\varepsilon_p+\hbar^2Q^2/M)$. Defining now $\mathbf{K}=\mathbf{K}_i-\mathbf{K}_j$ and introducing the quantities

$$\alpha=K^2/2-M\varepsilon_p/\hbar^2,$$

$$\Delta=K^2(K^2/4-M\varepsilon_p/\hbar^2),$$

$$Q_\pm^2=\alpha\pm\sqrt{\Delta},\tag{A2}$$

one can reformulate the integral as

$$S=2\int_0^\infty\frac{Q\,dQ}{4\pi^2}|b_e(Q)|^2$$

$$\times\begin{cases}\dfrac{2M}{\hbar^2\sqrt{-(Q^2-Q_-^2)(Q^2-Q_+^2)}} & \text{if } Q^2\in\,]Q_-^2,Q_+^2[\\ 0 & \text{if } Q^2\notin\,]Q_-^2,Q_+^2[\end{cases}$$

when $\Delta>0$ or $K^2>4M\varepsilon_p/\hbar^2$ and

$$S=0$$

when $\Delta<0$ or $K^2<4M\varepsilon_p/\hbar^2$. The sum S results

$$S(K)=\frac{2M}{\hbar^2}\int_{Q_-^2}^{Q_+^2}\frac{dQ^2}{4\pi^2}\frac{|b_e(Q)|^2}{\sqrt{-(Q^2-Q_-^2)(Q^2-Q_+^2)}}$$

when $K^2>4M\varepsilon_p/\hbar^2$.

Taking successively $Q^2=a+X\sqrt{\Delta}$ and $X=\cos x$, we deduce the form

$$S(K)=\frac{M}{2\pi\hbar^2}\int_0^\pi\frac{dx}{\pi}|b_e(Q=\sqrt{\alpha+\sqrt{\Delta}\,\cos x})|^2\tag{A3a}$$

when $K^2>4M\varepsilon_p/\hbar^2$ and

$$S=0\tag{A3b}$$

when $K^2<4M\varepsilon_p/\hbar^2$.

(iii) *The reaction constant* [Eq. (24)] is written as follows:

$$k(\varepsilon_p)=\frac{2\pi}{\hbar}(4\pi\beta)^2\sum_{(\mathbf{K}_i,\mathbf{K}_j)^*}e^{-\beta(K_i^2+K_j^2)}S(|\mathbf{K}_i-\mathbf{K}_j|).$$

Notation $(\mathbf{K}_i,\mathbf{K}_j)^*$ means that summation is restricted to couples satisfying the condition $|\mathbf{K}_i-\mathbf{K}_j|>K_0$, where $K_0=0$ when $\varepsilon_p<0$ and $K_0=\sqrt{4M\varepsilon_p/\hbar^2}$ when $\varepsilon_p>0$. A more convenient formulation is

$$k(\varepsilon_p)=\frac{2\pi}{\hbar}(4\pi\beta)^2\sum_{\mathbf{K}_j}e^{-2\beta K_j^2}\sum_{(\mathbf{K})^*}e^{-2\beta\mathbf{K}_j\cdot\mathbf{K}}e^{-\beta K^2}S(K)$$

$$=\frac{2\pi}{\hbar}(4\pi\beta)^2\int_{K_0}^\infty\frac{K\,dK}{2\pi}e^{-\beta K^2}S(K)$$

$$\times\int_0^\infty\frac{K_j dK_j}{2\pi}e^{-2\beta K_j^2}\int_0^{2\pi}\frac{d\theta}{2\pi}e^{-2\beta K_jK\cos\theta}$$

$$=\frac{2\pi}{\hbar}(4\pi\beta)^2\int_{K_0}^\infty\frac{K\,dK}{2\pi}e^{-\beta K^2}S(K)$$

$$\times\int_0^\infty\frac{K_j dK_j}{2\pi}e^{-2\beta K_j^2}J_0(2i\beta K_jK)$$

$$=\frac{2\pi}{\hbar}(4\pi\beta)^2\int_{K_0}^\infty\frac{K\,dK}{2\pi}e^{-\beta K^2}S(K)\,\frac{1}{8\pi\beta}\,e^{\beta K^2/2},\tag{A4}$$

where $J_0(x)$ is the Bessel function of the first kind. The reaction constant is expressed then as

$$k(\varepsilon_p)=\frac{\pi}{\hbar}\,\beta\int_{K_0^2}^\infty S(K)e^{-\beta K^2/2}dK^2.\tag{A5}$$

Considering (A3) and taking as a new variable $u=\beta K^2/2$ when $\varepsilon_p<0$ and $u=\beta K^2/2-\varepsilon_p/k_BT$ when $\varepsilon_p>0$, we obtain the result, which is correct regardless of the sign of ε_p:

$$k(\varepsilon_p)=k_0(|\varepsilon_p|)\times\frac{1}{1+\exp(\varepsilon_p/k_BT)},\tag{A6a}$$

with

$$k_0(|\varepsilon_p|)=\frac{M}{\hbar^3}(1+\exp-|\varepsilon_p|/k_BT)\int_0^\infty du\;e^{-u}\int_0^\pi\frac{dx}{\pi}\left|b_e\left(Q^2=\frac{u+|\varepsilon_p|/2k_BT+\cos x\sqrt{u(u+|\varepsilon_p|/k_BT)}}{\hbar^2/2Mk_BT}\right)\right|^2.\tag{A6b}$$

The form (A6b) respects the detailed balance principle. Calculation of k_0 involves a choice for the potential $b_e(r)$. Considering the asymptotic decrease of the envelope wave functions of excitons, we take the form

$$b_e(r)=b_{e0}e^{-r/\lambda\sqrt{2}}, \tag{A7a}$$

with the Fourier coefficient

$$b_e(Q)=\frac{4\pi\lambda^2 b_{e0}}{(1+2\lambda^2Q^2)^{3/2}}. \tag{A7b}$$

It leads to the form (we define the parameter $\varepsilon_\lambda=\hbar^2/2M\lambda^2$)

$$k_0(\varepsilon_p)=\frac{4\pi^2\hbar}{M}\frac{b_{e0}^2}{\varepsilon_\lambda^2}\frac{1+\exp-|\varepsilon_p|/k_BT}{(1+|\varepsilon_p|/\varepsilon_\lambda)^3}I(|\varepsilon_p|/\varepsilon_\lambda;|\varepsilon_p|/k_BT), \tag{A8a}$$

where $I(\zeta;\xi)$ is the following integral:

$$I(\zeta;\xi)=\int_0^\infty d(\xi y)e^{-\xi y}\int_0^\pi\frac{dx}{\pi}\left[\frac{1+\zeta[1+2y+2\sqrt{y(y+1)}\cos x]}{1+\zeta}\right]^{-3}=\int_0^\infty\frac{d(\xi y)e^{-\xi y}}{[1+4\zeta y/(1+\zeta)^2]^{3/2}}\frac{1+\zeta[1+2y+\sqrt{y(y+1)}/2]}{1+\zeta[1+2y+2\sqrt{y(y+1)}]}. \tag{A8b}$$

Here, $\zeta=|\varepsilon_p|/\varepsilon_\lambda$ and $\xi=|\varepsilon_p|/k_BT$; the following result has been used $(a>b)$:

$$\int_0^\pi\frac{dx}{\pi}(a+b\ \cos x)^{-3}=\frac{a+b/4}{a+b}(a^2-b^2)^{-3/2}.$$

The low-temperature limit is

$$\lim_{k_BT\to0}I(|\varepsilon_p|/\varepsilon_\lambda;|\varepsilon_p|/k_BT)=1.$$

Equation (A8) shows that the potential-energy variation in the transfer is paid by a reduction of the probability, *independent of the sign* of the variation: in the low-temperature limit, this reduction accounts for the factor $(1+|\varepsilon_p|/\varepsilon_\lambda)^{-3}$.

APPENDIX B

Renormalized exciton energies

In a mean-field approximation, the spin-spin coupling of any exciton (i) with all the others (j) is expressed by the following effective Hamiltonian:

$$\mathcal{H}^i=\sum_j\langle\mathbf{K}_j|^j\langle\psi|\mathcal{H}^{i,j}|\psi\rangle^j|\mathbf{K}_j\rangle$$

$$=\langle a_e\rangle s^i_{e,z}\sum_j{}^j\langle\psi|s^j_{e,z}|\psi\rangle^j+\langle a_h\rangle\tilde{s}^{\,i}_{h,z}\sum_j{}^j\langle\psi|\tilde{s}^{\,j}_{h,z}|\psi\rangle^j. \tag{B1}$$

Here $\mathcal{H}^{i,j}$ is defined by Eq. (3); $|\psi\rangle^j$ represents the spin state of exciton j; $\langle f\rangle=\int f(r)d^2r$, the integration extending over the unit area. Assuming a distribution N_θ of excitons on elliptic states $|\psi_\theta\rangle$ and densities $N_{\pm2}$ of excitons on states $|\pm2\rangle$, the calculation of the sums is straightforward. The result is

$$\mathcal{H}^i=\langle a_e\rangle[-N_{J=1}P_L+(N_2-N_{\bar2})]s^i_{e,z}+\langle a_h\rangle[N_{J=1}P_L+(N_2-N_{\bar2})]\tilde{s}^{\,i}_{h,z}. \tag{B2}$$

As an example, the self-energy of exciton i occupying a state $|+1\rangle$ in a gas of N excitons j occupying states $|-1\rangle$ is obtained with $N_{J=1}=N$, $N_2=N_{\bar2}=0$, and $P_L=-1$. One then finds

$${}^i\langle1|\mathcal{H}^i|1\rangle^i=\langle a_e\rangle N^i\langle1|s^i_{e,z}|1\rangle^i-\langle a_h\rangle N^i\langle1|\tilde{s}^{\,i}_{h,z}|1\rangle^i=-(\langle a_e\rangle+\langle a_h\rangle)N.$$

Since exciton i does not sustain any Pauli repulsion in this situation, the effective Hamiltonian measures the net Pauli repulsion energy experienced by the exciton i in any case if its energy origin is shifted by

$$(\langle a_e\rangle+\langle a_h\rangle)N\equiv(\langle a_e\rangle+\langle a_h\rangle)(N_{J=1}+N_2+N_{\bar2}).$$

This gives the renormalized effective Hamiltonian:

$$\mathcal{H}^i=[\langle a_e\rangle(1-P_Ls^i_{e,z})+\langle a_h\rangle(1+P_L\tilde{s}^{\,i}_{h,z})]N_{J=1}+[\langle a_e\rangle s^i_{e,z}+\langle a_h\rangle\tilde{s}^{\,i}_{h,z}](N_2-N_{\bar2})+(\langle a_e\rangle+\langle a_h\rangle)(N_2+N_{\bar2}). \tag{B3}$$

The Pauli repulsion energy of exciton $|\psi_\theta\rangle$ and $|\pm2\rangle$ are, respectively (first-order approximation),

$$\mathcal{E}_\theta={}^i\langle\psi_\theta|\mathcal{H}^i|\psi_\theta\rangle^i=[\langle a_e\rangle+\langle a_h\rangle](1+P_L\ \sin2\theta)N_{J=1}-[\langle a_e\rangle-\langle a_h\rangle]\times\sin2\theta(N_2-N_{\bar2})+[\langle a_e\rangle+\langle a_h\rangle](N_2+N_{\bar2}),$$

$$\mathcal{E}_{\pm2}={}^i\langle\pm2|\mathcal{H}^i|\pm2\rangle^i=[\langle a_e\rangle(1\mp P_L)+\langle a_h\rangle(1\pm P_L)]N_{J=1}+2[\langle a_e\rangle+\langle a_h\rangle]N_{\pm2}. \tag{B4}$$

[1] N. Peyghambarian, H. M. Gibbs, J. L. Jewell, A. Antonetti, A. Migus, D. Hulin, and A. Mysyrowics, Phys. Rev. Lett. **53**, 2433 (1984).
[2] D. Hulin, A. Mysyrowics, A. Antonetti, A. Migus, W. T. Mazzelink, H. Morkoc, H. M. Gibbs, and N. Peyghambarian, Phys. Rev. B **33**, 4389 (1986).
[3] S. Schmitt-Rink, D. S. Chemla, and D. A. B. Miller, Phys. Rev. B **32**, 6601 (1985).
[4] T. C. Damen, L. Vina, J. E. Cunningham, J. Shah, and L. J. Sham, Phys. Rev. Lett. **67**, 3432 (1991).
[5] B. Dareys, X. Marie, T. Amand, J. Barrau, Y. Shekun, I. Razdobreev, and R. Planel, Superlatt. Microstruct. **13**, 353 (1993).
[6] M. J. Snelling, P. Perozzo, D. C. Hutchings, I. Galbraith, and A. Miller, Phys. Rev. B **49**, 17 160 (1994).
[7] J. B. Stark, W. H. Knox, and D. S. Chemla, Phys. Rev. B **46**, 7919 (1992).
[8] T. Amand, X. Marie, B. Baylac, B. Darreys, J. Barrau, M. Brousseau, R. Planel, and D. J. Dunstan, Phys. Lett. A **193**, 105 (1994).
[9] D. Robart, T. Amand, X. Marie, B. Baylac, J. Barrau, M. Brousseau, and R. Planel, Symposium Benoît a la Guillaume, Paris, April, 1995 [Ann. Phys. (Paris) Suppl. **20**, C2-91 (1995)].
[10] A. Vinattieri, J. Shah, T. C. Damen, D. S. Kim, L. N. Pfeiffer, and L. J. Sham, Solid State Commun. **88**, 189 (1993).
[11] B. Sermage, B. Deveaud, S. Katzke, F. Clerot, C. Dumas, N. Roy, D. S. Katzer, F. Mollot, R. Planel, M. Berz, and J. C. Oudar, Superlatt. Microstruct. **13** (1993).
[12] H. Wang, J. Shah, T. C. Damen, and L. N. Pfeiffer, Phys. Rev. Lett. **74**, 3065 (1995).
[13] E. Hanamura, Phys. Rev. B **38**, 1228 (1988); L. Andreani and F. Bassani, Solid State Commun. **77**, 641 (1991).
[14] H. Wang, J. Shah, T. C. Damen, and L. N. Pfeiffer, *Ultra-fast Phenomena*, edited by W. H. Knox *et al.* (Springer-Verlag, Berlin, 1995).
[15] Y. Yamada, T. Mishina, Y. Masumoto, Y. Kawakami, S. Yamaguchi, K. Ichino, S. Fujita, S. Fujita, and T. Taguchi, Superlatt. Microstruct. **15**, 33 (1994).
[16] D. Robart, T. Amand, X. Marie, M. Brousseau, J. Barrau, and G. Bacquet, J. Opt. Soc. Am. B **13**, 1000 (1996).
[17] B. Sermage, S. Long, B. Deveaud, and D. S. Katzer, Third International Conference on Optics of Excitons in Confined Systems [J. Phys. (France) IV **3**, C5-10 (1993)].
[18] R. Eccleston, B. F. Feuerbacher, J. Kuhl, W. W. Rühle, and K. Ploog, Phys. Rev. B **45**, 11 403 (1992).
[19] D. S. Kim, T. Shah, T. C. Damen, W. Schäfer, F. Jahnke, S. Schmitt-Rink, and K. Köhler, Phys. Rev. Lett. **18**, 2725 (1992); S. Schmitt-Rink, Shaal Mukamel, K. Leo, J. Shah, and D. S. Chemla, Phys. Rev. A **44**, 2124 (1991).
[20] H. Wang, K. Ferrio, D. G. Steel, Y. Z. Hu, R. Binder, and S. W. Koch, Phys. Rev. Lett. **71**, 1261 (1993).
[21] K. Bott, O. Heller, D. Bennhardt, S. T. Cundiff, P. Thomas, E. J. Mayer, G. O. Smith, R. Eccleston, J. Kuhl, and K. Ploog, Phys. Rev. B **48**, 17 418 (1993); E. J. Mayer, G. O. Smith, V. Heuckeroth, J. Kuhl, K. Bott, A. Schulze, T. Meier, S. W. Koch, P. Thomas, R. Hey, and K. Ploog, *ibid*. **51**, 10 909 (1995).
[22] J. Y. Bigot, M. A. Mycek, S. Weiss, R. G. Ulbrich, and D. S. Chemla, Phys. Rev. Lett. **70**, 3307 (1993).
[23] M. Z. Maialle, E. A. de Andrada e Silva, and L. J. Sham, Phys. Rev. B **47**, 15 776 (1993).
[24] G. L. Bir, A. G. Aronov, and G. E. Pikus, Zh. Eksp. Teor. Fiz. **69**, 1382 (1975) [Sov. Phys. JETP **42**, 705 (1976)].
[25] For an excellent review on noninteracting excitons, see M. M. Denisov and V. P. Makarov, Phys. Status Solidi B **56**, 9 (1973).
[26] R. Knox, in *Solid State Physics: Advances in Research and Applications*, edited by F. Seitz and D. Turnbull (Academic, New York, 1963), Vol. 15, Suppl. 5.
[27] G. E. Pikus and G. L. Bir, Zh. Eksp. Teor. Fiz. **60**, 195 (1971) [Sov. Phys. JETP **33**, 108 (1971)].
[28] V. A. Kiselev and A. G. Zhilich, Fiz. Tverd. Tela (Leningrad) **13**, 2398 (1971) [Sov. Phys. Solid State **13**, 2008 (1972)].
[29] M. I. D'yakonov and V. I. Perel', Zh. Eksp. Teor. Fiz. **60**, 1954 (1971) [Sov. Phys. JETP **33**, 1053 (1971)].
[30] R. J. Elliot, Phys. Rev. **96**, 266 (1954); Y. Yaffet, *Solid State Physics: Advances in Research and Applications* (Academic, New York, 1963), Vol. 14, p. 1.
[31] T. Amand, B. Dareys, B. Baylac, X. Marie, J. Barrau, M. Brousseau, D. J. Dunstan, and R. Planel, Phys. Rev. B **50**, 11 624 (1994).
[32] T. C. Damen, J. Shah, D. Y. Oberli, D. S. Chemla, J. E. Cunningham, and J. M. Kuo, J. Lumin. **45**, 181 (1990); T. C. Damen, Karl Leo, J. Shah, and J. E. Cunningham, Appl. Phys. Lett. **58**, 1902 (1991).
[33] M. Colocci, M. Gurioli, and J. Martinez-Pastor, Third International Conference on Optics of Excitons in Confined Systems [J. Phys. (France) IV **3**, C5-10 (1993)].
[34] R. T. Phillips, D. J. Lovering, D. J. Denton, and G. W. Smith, Phys. Rev. B **45**, 4308 (1992).
[35] D. J. Lovering, R. T. Phillips, D. J. Denton, and G. W. Smith, Phys. Rev. Lett. **68**, 1880 (1992).
[36] J. C. Kim, D. R. Wake, and J. P. Wolfe, Phys. Rev. B **50**, 15 099 (1994).
[37] On the other hand, the first term in Eq. (4a) indicates that exciton-exciton exchange interaction results also in the transfer to the cross-polarized states which can explain the fast appearance of the cross-polarized signal in linearly polarized excitation experiments at high density.
[38] R. Planel and C. Benoît à la Guillaume, in *Optical Orientation*, edited by V. M. Agranovich and A. A. Maradudin, Modern Problems in Condensed Matter Sciences Vol. 8 (North-Holland, Amsterdam, 1984), p. 353. To our knowledge, these authors were the first to attribute the instability of linearly polarized exciton phases, in which neither the electron nor the hole have well-defined spins, to the exciton-exciton exchange interaction.
[39] E. Blackwood, M. J. Snelling, R. T. Harley, S. R. Andrews, and C. T. B. Foxon, Phys. Rev. B **30**, 14 246 (1994).
[40] T. Takagahara, Phys. Rev. B **31**, 6552 (1985).
[41] L. Landau and E. Lifchitz, *Mécanique Quantique* (Mir, Moscow, 1966), p. 257.
[42] M. Gurioli, A. Vinattieri, J. Martinez-Pastor, and M. Colocci, Phys. Rev. B **50**, 11 817 (1996).